

Advances in Spectrum Sensing and Cross-Layer Design for Cognitive Radio Networks*

Seung-Jun Kim, Emiliano Dall’Anese, Juan Andrés Bazerque, Ketan Rajawat,
and Georgios B. Giannakis[†]

Abstract

Spectrum sensing is the key task for cognitive radio (CR) networks with significant challenges that have attracted a flux of research and innovation in recent years. Various signal processing, learning and optimization techniques have been employed to tackle different aspects. In this paper, progresses made in this area are reviewed with emphasis on cross-layer design issues. The recent spectrum cartography techniques that capture the spatio-temporal RF environment in which the CRs operate is described in detail for physical layer sensing. MAC layer issues of scheduling the sensing operation based on the observation history are also outlined. The trade-off between sensing accuracy and the system-wide objective is highlighted in the context of sequential sensing schemes. The cross-layer benefit of rich cognition modalities toward network-wide performance is illustrated, and promising research directions are pointed out.

Submitted: November 15, 2011. Revised: August 29, 2012.

*This work was supported by QNRF grant NPRP 09-341-2-128.

[†]Corresponding author. The authors are with the Dept. of ECE, University of Minnesota, 200 Union Street SE, Minneapolis, MN 55455, U.S.A. Tel./Fax: (612)624-9510/625-2002, E-mails: {seungjun,emiliano,bazer002,ketan,georgios}@umn.edu.

GLOSSARY

cognitive radio: An intelligent radio that can learn and adapt to the environment.

primary user: A radio system that possesses an exclusive license to use a given spectrum band.

Neyman-Pearson test: A hypothesis test that maximizes the detection probability while ensuring a given false alarm probability.

physical (PHY) layer: A layer in the networking protocol stack concerned with electrical or optical interface to the communication medium.

medium access control (MAC) layer: A layer in the networking protocol stack concerned with sharing a physical connection among multiple communication entities.

cross-layer design: A design approach for networking protocols that takes into account interactions among different layers in the protocol stack.

NOMENCLATURE

$\Phi(\mathbf{x}, f)$: power spectral density (PSD) at position \mathbf{x} and frequency f

$\varphi(\mathbf{x}, f)$: measured PSD at position \mathbf{x} and frequency f

$\hat{\Phi}(\mathbf{x}, f)$: estimated PSD at position \mathbf{x} and frequency f

$\Phi_s(f)$: transmit-PSD of source s at frequency f

$g_{\mathbf{x}_s \rightarrow \mathbf{x}_r}(t, f)$: gain of the channel from position \mathbf{x}_s to position \mathbf{x}_r at time t and frequency f

$\boldsymbol{\theta}$: vector of basis expansion coefficients for the PSD map

\mathbf{x}_r : position of the r -th CR

N_r : number of CRs

N_g : number of grid points

N_b : number of known bases

$\boldsymbol{\theta}_g$: the g -th group of basis expansion coefficients

N : number of samples

$s_{\mathbf{x} \rightarrow \mathbf{x}_s}$: shadow fading of the channel from position \mathbf{x} to position \mathbf{x}_s

$\ell(\mathbf{x}, t)$: spatial loss field at position \mathbf{x} and time t

I. INTRODUCTION

The cognitive radio (CR) paradigm endeavors to mitigate the scarcity of spectral resources for wireless communication through intelligent sensing and agile resource allocation techniques (Mitola III and Maguire, Jr., 1999; Haykin, 2005). The motivating reason is that although most of the available spectrum has been licensed to primary users (PUs) for exclusive usage, it is often significantly underutilized depending on the time and the location that communication takes place (FCC Spectrum Policy Task Force, 2002). The CRs aim to learn the RF landscape, and identify the unused spectral resources—often called “white space” or “spectrum holes”—in the time, frequency, and space domains through spectrum sensing. Based on the information obtained, judicious resource management is then performed to communicate opportunistically without causing harmful interference to the licensed PU systems.

The sensing task can be as basic as detecting the presence of PU signals in a given band at a given time. It can become as sophisticated as estimating the channel gains, transmit-powers, modulation classes, and PU locations, as well as learning their traffic patterns. Deciding the PU presence is necessary for the *spectrum overlay* scenario (Zhao and Sadler, 2007), in which the CRs identify completely unoccupied bands to transmit on. Channel gains between CR transmitters and PU receivers are useful for interference control in the *spectrum underlay* scenario, in which the CRs are allowed to share bands with the PUs, provided that the interference experienced by the PUs is maintained below an acceptable level. The bottom line is that the richer the information collected on the PU systems and the surrounding RF environment, the more adaptable the CR operation can become via dynamic resource optimization.

Spectrum sensing is no easy task. The CRs often need to scan a huge swath of bandwidth in order to identify spectrum holes (Tian and Giannakis, 2007). In the prevalent case of no cooperation occurring between PU and CR systems, the PU signals must be detected in a low signal-to-noise power ratio (SNR) regime. The lack of dedicated training signals may render it difficult for the CR systems to acquire the channels accurately. In fact, the CRs might not even have prior knowledge on the PU signal characteristics, often limiting the options to using simple energy detectors (radiometers) (Pawelczak et al., 2011). Thus, obtaining a decent detection performance can become quite challenging (Tandra and Sahai, 2008). The difficulty is only aggravated with the hidden terminal issues and strenuous propagation environments which may include fading and shadowing (Unnikrishnan and Veeravalli, 2008).

These formidable challenges have invited intensive research in this area. At the physical layer, various *cooperative* sensing schemes have been developed to cope with the hidden terminal problems and combat fading through

diversity combining of the samples taken by multiple CRs (Ganesan and Li, 2005; Ghasemi and Sousa, 2007). Cyclostationarity detectors have been developed for improved sensing performance (Cabric et al., 2005; Lunden et al., 2009). Various signal processing and learning tools have been employed to effectively capture the RF environment in which the CR network is deployed (Alaya-Feki et al., 2008; Bazerque and Giannakis, 2010; Kim et al., 2011a). To minimize sensing delay while meeting the detection performance targets, sequential detectors have been investigated (Chaudhari et al., 2009; Kim and Giannakis, 2010). Both parallel scanning of multiple bands as well as serial search have been considered (Quan et al., 2009; Fan and Jiang, 2010). In the case of serial search, selecting the bands to sense and coordinating the search along with the access among multiple CRs have attracted much research toward designing the MAC layer tailored for CR sensing (Zhao et al., 2007; Ahmad et al., 2009; Cheng and Zhuang, 2011).

It is largely part of ongoing research how to effectively permeate the benefits of enhanced cognition capability of the CRs to cross-layer network design and adaptation. Needless to say, this is of critical importance for efficient, reliable, quality-of-service-assuring operation of CR networks in the presence of dynamics and uncertainties in the CR deployment (Shiang and van der Schaar, 2009). It has been recognized that the sensing algorithms must be designed with the cross-layer interaction in mind (Liang et al., 2008; Wang et al., 2009). This tutorial paper aims to survey some of the advances made in CR spectrum sensing, and also highlight the intertwined cross-layer resource management issues, hopefully providing with fruitful directions for future research.

The organization of the rest of the paper is as follows. An overview of the physical layer sensing techniques are provided in Sec. II with emphasis on the recent RF cartography approaches. The MAC layer issues of sensing is briefly reviewed in Sec. III. The implications of sensing to cross-layer design are illustrated in Sec. IV. Some conclusions are offered in Sec. V.

II. SENSING AT THE PHYSICAL LAYER

Signal detection is the core element of CR sensing, with Neyman-Pearson (NP) hypothesis testing offering the natural and most widely used framework. With the objective of deciding whether a PU is present or white space is available, the CR acquires samples of the ambient RF signal $x(t)$ and decides between two hypotheses: $H_0 : x(t) = n(t)$ versus $H_1 : x(t) = s(t) + n(t)$, where $n(t)$ denotes ambient noise and $s(t)$ a PU signal

possibly affected by multipath and shadow fading effects. The *energy detection* is widely used because it is simple and does not require knowledge about the PU system parameters (Pawelczak et al., 2011). The test statistic (TS) $S_T = \sum_{t=1}^T x^2(t)$ is modeled as χ^2 -distributed assuming that the noise variance is known. In order to avoid self interference, multiple CRs competing for the same bands must schedule quiet periods, that is, time intervals where CRs suspend transmission and perform detection (Cordeiro et al., 2005).

Modulated signals are typically cyclostationary processes, that is, their correlation function $r(t, \tau) := \mathbb{E}\{x(t)x^*(t-\tau)\}$ is periodic in t , which implies that its Fourier spectrum peaks at the cyclic frequency corresponding to its period. *Cyclostationarity detection* capitalizes on this property to detect a PU signal even in low SNR, since white noise yields zero correlation at nonzero lags regardless of its power level (Lunden et al., 2009). Furthermore, cyclostationarity detectors can separate signals with different cyclic frequencies, thus potentially not requiring quiet periods. These advantages come at the price of requiring larger data records to attain comparable performance relative to energy detection, since cyclostationarity detection entails sample estimates of the fourth-order moments.

Standard NP tests predefine the number of samples to acquire as a function of prescribed test performance, i.e., the probabilities of detection and false alarms. *Sequential alternatives* are available, in which the TS is updated sample by sample (Choi et al., 2009). Depending on how informative this TS is, three actions are possible, namely, rejecting the null or the alternative hypotheses, or acquiring an additional sample. For a specified test performance, the technique is proven to reduce the number of required samples in average, although it may exceed the NP sample size on a bad realization.

In wideband sensing, the CRs often need to scan different bands in search for white space. These bands can be tested independently by applying single-band detectors separately. In *multi-band testing*, decision thresholds corresponding to different bands can be optimized jointly (Quan et al., 2009). Accordingly, the test performance is not prescribed but designed to maximize the aggregate CR throughput across frequency bands. Increasing the thresholds increases the chance of CR transmissions, increasing the throughput. It also increases the probability of miss detection. This probability is controlled by setting a price for interfering with PUs, and prescribing an upper bound to the aggregate cost across bands that the CR can afford (Quan et al., 2009). A compressive sampling approach has also been proposed for inspecting all bands together at sub-Nyquist sampling rates (Zeng et al., 2011).

Collaboration among CRs adds spatial diversity to the sensing methods which is crucial for improved detection

of white spaces, since shadowing effects may lead a single CR to miss detection (Unnikrishnan and Veeravalli, 2008). In particular, the hidden terminal problem can be mitigated by collaboration. Such a situation arises when a CR is not in the range of a PU transmitter, but a PU receiver in-between falls in the range of the CR. In this setup, the CR will miss the PU transmitter, infer white space, and start communicating, thus causing harmful interference to the PU receiver. In addition to gaining spatial diversity, collaborative CRs can share sensing resources with the potential to reduce sensing time or to improve detection performance (Ganesan et al., 2008).

Cooperation protocols must be judiciously designed so that the overhead introduced for collaboration does not outweigh the increase in the throughput of the opportunistic access (Ghasemi and Sousa, 2007). Centralized CR networks are often considered, with CRs communicating their TSs to a fusion center (FC), where these are combined to yield a fused decision. Combining unquantized (i.e., soft) TSs serves as a guideline for the design of optimal protocols (Quan et al., 2008; Ma et al., 2008). However, quantization is important for striking a balance in the data transmission-sensing trade-off. To this end, schemes combining quantized TSs have been proposed, even with one-bit resolution (Zhang et al., 2009).

Distributed processing offers an alternative to the FC-based cooperation. Information is shared among neighboring CRs only, a preferable architecture for large networks since long-range communication to an FC consumes excessive power and interferes with reports from all other CRs in the network. In addition, *decentralized* networks are more robust since their operation is not dependent on a single point of failure, and it is more flexible since an entering CR only needs to discover its neighbors to start operating without competing for access to the FC. The information shared in the neighborhood eventually percolates across the entire network after a number of local communication steps, and approaches the optimality of a centralized CR network (Bazerque and Giannakis, 2010).

Optimality here should be understood as achieving the prescribed test performance with minimal number of samples, or maximizing the throughput. These criteria are “socially optimal” for the CR network. *Game theoretic* approaches have also been proposed in which a single CR decides whether or not to sense and collaborate in order to maximize its own throughput (Wang et al., 2010). A CR might decide not to sense and use its resources to transmit on available bands according to the sensing results of its peer CRs. This strategy is not optimal if followed by all CRs as no white spaces are revealed, and then individual CRs are compelled to sense the spectrum. A strategy is developed in (Wang et al., 2010) to achieve a stable equilibrium point in which CRs balance sensing

and transmission times.

Censoring offers a complementary approach to quantization when it comes to reducing the overhead. Since communicating local TSs consumes energy and bandwidth, the CRs are allowed to do so only when S_T is sufficiently informative. A two-threshold approach was proposed in (Maleki et al., 2011), where the CRs transmit S_T only when it is below the lower threshold, or above the higher one. The thresholds are designed to guarantee the prescribed test performance, considering the cost of sensing and TS transmission (Maleki et al., 2011).

These multiple dimensions of the CR sensing problem are summarized in Fig. 1, and overviewed more extensively in the tutorial reference (Akyildiz et al., 2011). Recently, *spectrum cartography* opened a new dimension for CR sensing by analyzing the spectral opportunities not only in frequency but also in space (Alaya-Feki et al., 2008; Bazerque and Giannakis, 2010; Kim et al., 2011a). The underlying departure of these approaches relative to the conventional sensing algorithms is that the PU's band occupancy is no longer deemed the same regardless of location. Rather, spectrum cartography sets the objective of revealing a map of the spectrum occupancy across space per frequency band. Estimating spectrum

Energy	Cyclostationarity
Single-band	Multi-band
Fixed-sample size	Sequential
FC-based	Decentralized
Socially optimal	Game-theoretic
Soft-combined	Hard-combined
Censored	Uncensored
Space-invariant	Cartography

Fig. 1. Aspects of collaborative CR sensing at the physical layer

maps is particularly relevant for wide-area ad-hoc networks, where PU transmissions typically reach only a small subset of CRs. Knowing the spectrum across space allows remote CRs to reuse idle bands. It also enables the CRs to adapt their transmit-powers or positions to minimally interfere with PUs (Wang et al., 2011). Of course, more sophisticated sensing approaches demand higher implementation complexity. While a viable alternative may be to formally allow the CRs and the PUs collaborate, it is noted that the CR paradigm advocated here does not need to be confined to the CR networking per se, but may be instrumental to other complex wireless networking scenarios, where distributed and autonomous cognition of the environment is useful (Geirhofer et al., 2010). The cartography approach is described in more detail in the ensuing section.

A. Sparsity-Aware Power Spectrum Cartography

A parametric approach to cooperative RF cartography is developed in (Bazerque and Giannakis, 2010) with the goal of mapping out the ambient RF power levels in the geographical area $\mathcal{A} \subseteq \mathbb{R}^2$ of interest. The setup includes N_s sources (PU transmitters) located at position vectors $\{\mathbf{x}_s \in \mathcal{A}\}_{s=1}^{N_s}$, and N_r receivers (CRs) at locations $\{\mathbf{x}_r \in \mathcal{A}\}_{r=1}^{N_r}$. The transmit-power spectral density (PSD) of a source signal at position \mathbf{x}_s is represented by a basis expansion as $\Phi_s(f) = \sum_{\nu=1}^{N_b} \theta_{s\nu} b_\nu(f)$, where $\{b_\nu(f)\}_{\nu=1}^{N_b}$ is a collection of known bases, and $\{\theta_{s\nu}\}_{\nu=1}^{N_b}$ denotes the expansion coefficients to be estimated per source s . Assuming spatial uncorrelatedness of channels and sources, the PSD $\Phi(\mathbf{x}_r, f)$ measured at receiving CRs at $\{\mathbf{x}_r\}_{r=1}^{N_r}$ in the presence of white noise with respective variances $\{\sigma_r^2\}_{r=1}^{N_r}$ is expressed as

$$\Phi(\mathbf{x}_r, f) = \sum_{s=1}^{N_s} g_{\mathbf{x}_s \rightarrow \mathbf{x}_r} \Phi_s(f) + \sigma_r^2 = \sum_{s=1}^{N_s} g_{\mathbf{x}_s \rightarrow \mathbf{x}_r} \sum_{\nu=1}^{N_b} \theta_{s\nu} b_\nu(f) + \sigma_r^2 = \mathbf{b}_r^T(f) \boldsymbol{\theta} + \sigma_r^2 \quad (1)$$

where T denotes transposition; $g_{\mathbf{x}_s \rightarrow \mathbf{x}_r}$ the average channel gain of the $\mathbf{x}_s \rightarrow \mathbf{x}_r$ link; $\boldsymbol{\theta}$ the vector formed by stacking the columns of the matrix with entries $\theta_{s\nu}$; and $\mathbf{b}_r(f)$ the vector constructed by concatenating the columns of the matrix with (s, ν) -entry $g_{\mathbf{x}_s \rightarrow \mathbf{x}_r} b_\nu(f)$. One possible choice for the channel gains is to adopt an inverse polynomial path loss model so that $g_{\mathbf{x}_s \rightarrow \mathbf{x}_r}$ is only a function of the distance between \mathbf{x}_r and \mathbf{x}_s . Alternatively, estimates can be obtained from channel gain cartography, which will be explained in Sec. II-B.

Given PSD measurements $\{\varphi(\mathbf{x}_r, f_n)\}_{n=0}^{N-1}$ at N discrete frequencies per CR r , the goal is to estimate the *PSD maps* $\hat{\Phi}(\mathbf{x}, f) \forall \mathbf{x} \in \mathcal{A}$, one per frequency f . From the linear model (1), this is possible provided an estimate of $\boldsymbol{\theta}$ becomes available.

1) *Compressed sensing approach*: Let $\boldsymbol{\varphi}_r$ denote the $N \times 1$ vector with the n -th entry $\varphi_{rn} := \varphi(\mathbf{x}_r, f_n)$ representing the PSD measurement obtained, e.g., by sample-average on periodograms. Defining the estimation error vector \mathbf{e}_r likewise, one arrives at the local vector-matrix model per CR r

$$\boldsymbol{\varphi}_r = \mathbf{B}_r \boldsymbol{\theta} + \mathbf{e}_r, \quad r = 1, 2, \dots, N_r \quad (2)$$

where matrix \mathbf{B}_r is formed to have rows $\{\mathbf{b}_r^T(f_n)\}_{n=1}^N$, and the noise variance is absorbed in $\boldsymbol{\varphi}_r$ or $\boldsymbol{\theta}$ without loss of generality.

Cooperative PSD sensing is possible because $\boldsymbol{\theta}$ is common to all N_r receiving CRs. This allows estimation of

θ in the linear regression model (2) using the nonnegative (NN), and thus non-linear, LS criterion

$$\min_{\theta \geq 0} \sum_{r=1}^{N_r} \left\| \varphi_r - B_r \theta \right\|^2 \quad (3)$$

where the nonnegativity constraints are naturally imposed to prevent negative PSD estimates.

With position vectors \mathbf{x}_s (and/or \mathbf{x}_r) unknown, even the model in (1) is nonlinear and the NN-LS optimization in (3) is rendered non-convex with multiple local minima. To bypass this challenge, the idea in (Bazerque and Giannakis, 2010) relies on a virtual grid of N_g candidate source locations as the one depicted in Fig. 2. Vectors \mathbf{x}_s are replaced by \mathbf{x}_g in Fig. 2, which no longer describe the actual positions of the PUs, but rather the grid points with *known* spatial coordinates where the PUs could be present. This virtual grid model removes the model nonlinearity, while rendering (3) convex at the price of the increased number of unknowns. Aided by the virtual grid,

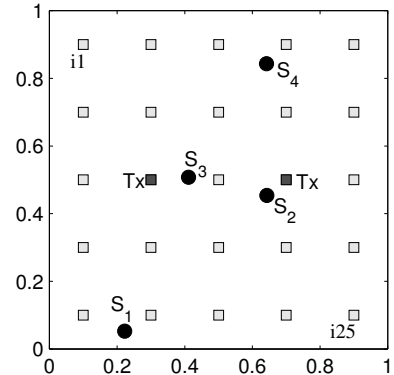


Fig. 2. Virtual CR network grid.

one can in principle obtain the PU locations that best fit the measurements via exhaustive search, provided that the number of PUs is known. (The number of PUs may be determined from model complexity, e.g., using Akaike's information-theoretic criterion.)

The exhaustive search is clearly undesirable because it incurs combinatorial complexity that grows rapidly in the number of grid points. In fact, a dense grid may be preferred to achieve higher precision in localizing the PUs. Recent advances in compressive sampling can mitigate this hurdle by exploiting the sparsity present in θ (Candès and Plan, 2009; Chen et al., 1998; Tibshirani, 1996). Sparsity is manifested because individual transmissions typically occupy only a small fraction of the possibly huge system bandwidth. Moreover, active PUs are present only at a small fraction of candidate locations $\{\mathbf{x}_g\}$.

In particular, the least-absolute shrinkage and selection operator (Lasso) (Tibshirani, 1996), also known as denoising basis pursuit (Chen et al., 1998), amounts to augmenting (3) with the ℓ_1 norm $\|\theta\|_1 := \sum_{s=1}^{N_g} \sum_{\nu=1}^{N_b} |\theta_{s\nu}|$ weighted by a sparsity-tuning parameter λ_1 . After incorporating PSD-imposed nonnegativity constraints, the Lasso for PSD map estimation amounts to solving the following convex optimization problem

$$\hat{\theta} = \arg \min_{\theta \geq 0} \sum_{r=1}^{N_r} \left\| \varphi_r - B_r \theta \right\|_2^2 + \lambda_1 \|\theta\|_1. \quad (4)$$

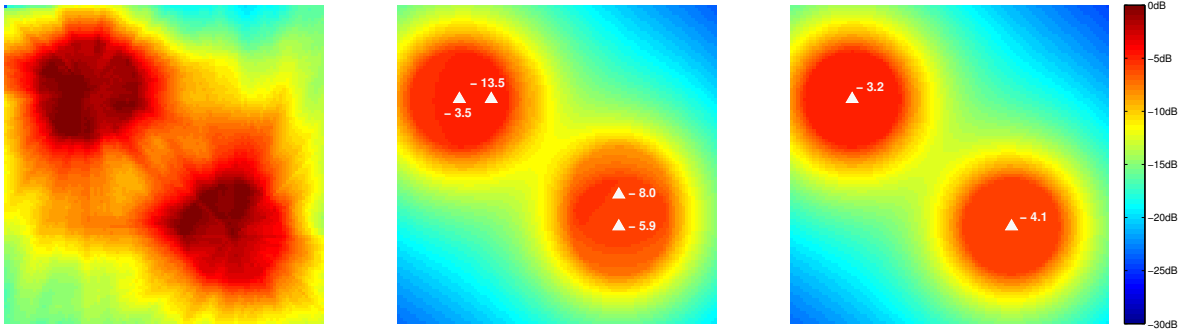


Fig. 3. (left) PSD map generated by two sources in 6dB of log-normal shadowing aggregated across frequency; (center) estimate obtained from (5) with $N_r = 50$ and $N_g = 100$; (right) robust estimate (6).

Clearly, the larger λ_1 is chosen, the more entries of $\hat{\boldsymbol{\theta}}$ will be shrunk to zero. The remaining non-zero entries of $\hat{\boldsymbol{\theta}}$ yield the positions and power of active transmitters, the bands used for transmission, and eventually the entire PSD map $\hat{\Phi}(\mathbf{x}, f) \forall f$ and $\forall \mathbf{x} \in \mathcal{A}$ [cf. (1)].

2) *Sparsity at group and coefficient levels:* A refinement of the estimator in (4) is obtained by observing the hierarchical sparsity present in $\boldsymbol{\theta}$: when a point \mathbf{x}_g is unoccupied by a PU transmitter, the entire basis expansion coefficients $\boldsymbol{\theta}_g := [\theta_{g1}, \dots, \theta_{gN_b}]^T$ corresponding to this point would become zero. On this account, the regularizer in (4) is augmented by adding the term $\lambda_2 \sum_{g=1}^{N_g} \|\boldsymbol{\theta}_g\|_2$, which encourages sparsity at the group level (Yuan and Lin, 2006; Dall’Anese et al., 2012). The ℓ_1 penalty is preserved in order to promote sparsity at the single coefficient level in the surviving $\boldsymbol{\theta}_g$, accounting for the sparsity in the frequency domain, yielding

$$\hat{\boldsymbol{\theta}} = \arg \min_{\boldsymbol{\theta} \succeq \mathbf{0}} \frac{1}{2} \sum_{r=1}^{N_r} \|\boldsymbol{\varphi}_r - \mathbf{B}_r \boldsymbol{\theta}\|_2^2 + \lambda_1 \|\boldsymbol{\theta}\|_1 + \lambda_2 \sum_{g=1}^{N_g} \|\boldsymbol{\theta}_g\|_2. \quad (5)$$

The group penalty encourages sparsity at the group level, either by shrinking to zero all variables within a group, or by retaining them altogether. As λ_2 is increased, more group estimates $\boldsymbol{\theta}_g$ become zero.

3) *Uncertainty on the propagation model:* Further enhancement was introduced in (Dall’Anese et al., 2012) to achieve robustness against perturbations in matrices \mathbf{B}_r . Uncertainty in these matrices is due to: (i) errors in the estimates of $\{g_{\mathbf{x}_s \rightarrow \mathbf{x}_r}\}$; (ii) position offsets when PUs are located between grid points; and (iii) approximation errors in basis expansion. The resultant model mismatches are captured by an additive error matrix \mathbf{E} , yielding a perturbed model $\boldsymbol{\varphi} = (\mathbf{B} + \mathbf{E})\boldsymbol{\theta}$, where $\boldsymbol{\varphi}$ is obtained by stacking vectors $\boldsymbol{\varphi}_r$, and \mathbf{B} by stacking matrices \mathbf{B}_r .

Under this new model, it is pertinent to adopt a total LS formulation (Zhu et al., 2011; Dall’Anese et al., 2012)

$$\{\hat{\boldsymbol{\theta}}, \hat{\mathbf{E}}\} = \arg \min_{\mathbf{E}, \boldsymbol{\theta} \succeq \mathbf{0}} \frac{1}{2} \|\boldsymbol{\varphi} - (\mathbf{B} + \mathbf{E}) \boldsymbol{\theta}\|_2^2 + \frac{1}{2} \|\mathbf{E}\|_F^2 + \lambda_1 \|\boldsymbol{\theta}\|_1 + \lambda_2 \sum_{g=1}^{N_g} \|\boldsymbol{\theta}_g\|_2. \quad (6)$$

Fig. 3 shows how (5) is capable of recovering the PSD maps across space under log-normal shadowing, and how its robust version (6) is more effective on resolving sources located off the grid points. Estimator (6) can still be limited by fading, which is not accounted for in the model. A systematic method for identifying and rejecting such outliers can also be found in (Dall’Anese et al., 2012).

4) *Nonparametric basis pursuit*: A nonparametric basis pursuit method was applied to spectrum cartography in (Bazerque et al., 2011) and shown to offer a valuable augmentation of the parametric path loss model considered so far. The basis expansion model for the PSD maps is recast as

$$\Phi(\mathbf{x}, f) = \sum_{\nu=1}^{N_b} g_{\nu}(\mathbf{x}) b_{\nu}(f) \quad (7)$$

where $g_{\nu}(\mathbf{x})$ collects the aggregate power from all sources at receiving point \mathbf{x} . Without prescribing the functional form of $g_{\nu}(\mathbf{x})$ a priori, these functions are interpolated from the available data.

To capture the smooth variation of $\Phi(\mathbf{x}, f)$, the criterion for selecting $g_{\nu}(\mathbf{x})$ is regularized using the so-termed thin-plate penalty (Wahba, 1990, p. 30). Functions $\{g_{\nu}\}_{\nu=1}^{N_b}$ are estimated as

$$\{\hat{g}_{\nu}\}_{\nu=1}^{N_b} := \arg \min_{\{g_{\nu} \in \mathcal{S}\}} \frac{1}{N_r N} \sum_{r=1}^{N_r} \sum_{n=1}^N \left(\varphi_{rn} - \sum_{\nu=1}^{N_b} g_{\nu}(\mathbf{x}_r) b_{\nu}(f_n) \right)^2 + \lambda_s \sum_{\nu=1}^{N_b} \int_{\mathbb{R}^2} \|\nabla^2 g_{\nu}(\mathbf{x})\|_F^2 d\mathbf{x} \quad (8)$$

where $\|\nabla^2 g_{\nu}\|_F$ denotes the Frobenius norm of the Hessian of g_{ν} , and \mathcal{S} the space of Sobolev functions, for which the penalty is well defined (Duchon, 1977, p. 85). The parameter $\lambda_s \geq 0$ controls the degree of smoothing. Specifically, for $\lambda_s = 0$ the estimates in (8) correspond to *rough* functions interpolating the data; while as $\lambda_s \rightarrow \infty$ the estimates yield linear functions (i.e., $\nabla^2 \hat{g}_{\nu}(\mathbf{x}) \equiv \mathbf{0}_{2 \times 2}$). A smoothing parameter in-between these limiting values is selected using, e.g., the leave-one-out cross-validation approach; see e.g., (Hastie et al., 2009).

The optimization problem (8) is variational in nature, and in principle requires searching over the infinite-dimensional function space \mathcal{S} . Fortunately, it turns out that (8) admits closed-form, finite-dimensional minimizers

$$\hat{g}_{\nu}(\mathbf{x}) = \sum_{r=1}^{N_r} \beta_{\nu r} K(\|\mathbf{x} - \mathbf{x}_r\|_2) + \boldsymbol{\alpha}_{\nu 1}^T \mathbf{x} + \alpha_{\nu 0}, \quad \nu = 1, \dots, N_b \quad (9)$$

where $K(\rho) := \rho^2 \log(\rho)$, and $\boldsymbol{\beta}_{\nu} := [\beta_{\nu 1}, \dots, \beta_{\nu N_r}]^T$ satisfies $\sum_{r=1}^{N_r} \beta_{\nu r} = 0$, and $\sum_{r=1}^{N_r} \beta_{\nu r} \mathbf{x}_r = \mathbf{0}$. Optimal coefficients $\mathbf{c}_{\nu}^* := [\beta_{\nu 1}^*, \dots, \beta_{\nu N_r}^*, \boldsymbol{\alpha}_{\nu 1}^{*T}, \alpha_{\nu 0}^*]$ can be found by substituting (9) back into (8) and solving it.

5) *Group-Lasso on splines*: An improved spline-based PSD estimator can be obtained by exploiting group sparsity to fit unknown spatial functions $\{g_\nu\}_{\nu=1}^{N_b}$ using (7) with $N_b \gg N_r N$, possibly with an overcomplete set of bases $\{b_\nu\}_{\nu=1}^{N_b}$. The resultant model is particularly attractive when there is an inherent uncertainty on the PU transmission parameters, such as the center frequency or the pulse shape including the roll-off factor. Adaptive communication schemes frequently adjust such parameters (Goldsmith, 2005, Ch. 9). A sizable collection of bases can effectively accommodate most of the possible cases, providing model robustness. Thus, known bases are selected to describe frequency characteristics of the PSD map, while a variational approach is employed to capture spatial dependencies.

In this context, the envisioned estimation method provides the CRs with capability of selecting a few bases that better “explain” the actual transmitted signals. As a result, most functions g_ν are expected to be identically zero; hence, there is an inherent form of sparsity present that can be exploited to improve estimation. A major departure from the conventional basis pursuit (Chen et al., 1998) is that (7) entails bases weighted by functions $\{g_\nu\}$ rather than scalars.

The proposed nonparametric basis pursuit method amounts to obtaining $\{\hat{g}_\nu\}_{\nu=1}^{N_b}$ from φ_{rn} as

$$\begin{aligned} \{\hat{g}_\nu\}_{\nu=1}^{N_b} := \arg \min_{\{g_\nu \in \mathcal{S}\}} & \frac{1}{N_r N} \sum_{r=1}^{N_r} \sum_{n=1}^N \left(\varphi_{rn} - \sum_{\nu=1}^{N_b} g_\nu(\mathbf{x}_r) b_\nu(f_n) \right)^2 + \lambda_s \sum_{\nu=1}^{N_b} \int_{\mathbb{R}^2} \|\nabla^2 g_\nu(\mathbf{x})\|_F^2 d\mathbf{x} \\ & + \mu \sum_{\nu=1}^{N_b} \|[g_\nu(\mathbf{x}_1), \dots, g_\nu(\mathbf{x}_{N_r})]\|_2. \end{aligned} \quad (10)$$

Relative to (8), the cost in (10) is augmented with an additional regularization term weighted by a tuning parameter $\mu \geq 0$. Clearly, if $\mu = 0$, then (10) boils down to (8). To appreciate the role of the new penalty term, note that the minimization of $\|[g_\nu(\mathbf{x}_1), \dots, g_\nu(\mathbf{x}_{N_r})]\|_2$ intuitively shrinks all pointwise function values $\{g_\nu(\mathbf{x}_1), \dots, g_\nu(\mathbf{x}_{N_r})\}$

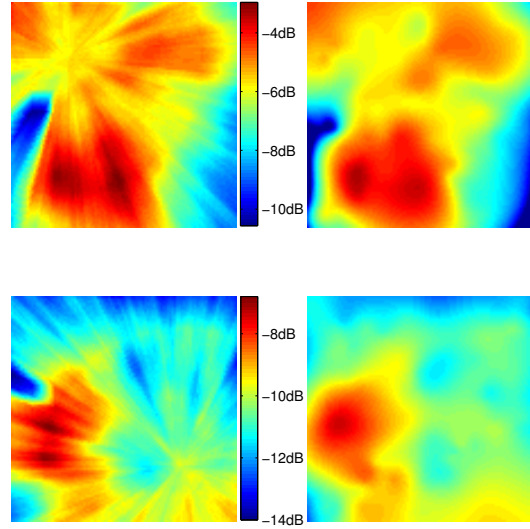


Fig. 4. (top) Power distribution across space with $g_6(\mathbf{x})$ in the band of 2437MHz; (top-left) actual distribution; (top-right) estimated map from $N_r = 100$ CRs. (Bottom) Power distribution across space with $g_{11}(\mathbf{x})$ in the band of 2462MHz; actual distribution and estimated map.

to zero for sufficiently large μ . Interestingly, it is shown in (Bazerque et al., 2011) that this suffices to guarantee that $\hat{g}_\nu(\mathbf{x}) \equiv 0 \forall \mathbf{x}$. This property is due to the fact that (9) still holds as a finite-dimensional solution to (10).

Fig. 4 exhibits the capability of this approach for recovering the PSD maps on the 6-th and 11-th channel of the PUs abiding by the IEEE 802.11 wireless LAN standard. Compared to (6), the nonparametric approach in (10) can cope with shadowing effects at the price of increasing the number of CR sensors.

There are a number of practical issues in implementing the cartography algorithms. First, the PSD cartography algorithms must be run in a time scale commensurate with the coherence times of the RF emitter activities that the maps intend to capture. Typical implementation constraints would probably render it infeasible to track packetized transmission bursts or very high mobility. On the other hand, slowly varying RF landscape can be tracked based on the RF energy measurements accumulated over an appropriate duration. Online versions of the cartography algorithms have been developed for such purposes (Bazerque and Giannakis, 2010; Bazerque et al., 2011). The subsequent subsection provides an alternative mapping idea, which may be useful in tracing fast-varying PU activities. In addition to the robustness against channel uncertainties obtained via the total LS approach described in Sec. II-A3, robustness of the PSD maps to the grid granularity was considered (Bazerque and Giannakis, 2010). Distributed synchronization as well as the position estimates of the CRs can be acquired via the GPS or other algorithms developed in the context of wireless sensor networking research.

B. Channel Gain Cartography

PSD cartography and PU localization algorithms are useful to identify regions that are “crowded” in terms of RF interference, and hence to be avoided by CR transmission. On the other hand, a complementary channel gain cartography is necessary to address the interference management issues in the spectrum underlay scenario. Channel coefficients and interference levels are generally acquired on a per-link basis by employing point-to-point training schemes. Although effective in conventional wireless networks, their application to the CR scenario is problematic due to the lack of cooperation between CR and PU nodes.

As a motivating example, consider the setup in Fig. 5(a), where a CR transmitter aims to spatially reuse the frequency bands occupied by the PUs. As PU and CR systems do not generally cooperate, the CR transmitter relies upon a simple path loss model to ensure PU protection; i.e., to guarantee that the interference inflicted to PU

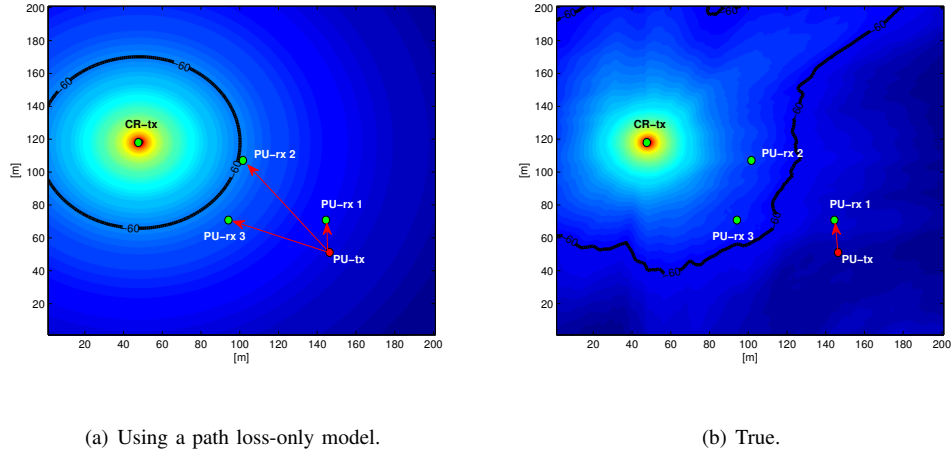


Fig. 5. Coverage region of a transmitter.

receivers does not exceed a prescribed threshold (Zhang, 2009; Zhao and Sadler, 2007), which is set to -60 dB in Fig. 5(a). However, due to random shadowing and small-scale propagation effects, employing a path loss-only model to calibrate the transmit-power may cause undesired disruption of PU communications (Kumaran et al., 2002), as depicted in Fig. 5(b). On the other hand, when significant signal attenuation exists due to shadowing, the CR links can benefit from it by raising the transmit-power levels. The key here is cognition of the spatio-temporal evolution of propagation channels.

Toward this end, a novel approach was recently put forth in (Kim et al., 2011a; Dall’Anese et al., 2011a), where the concept of *channel gain map* was introduced. For a CR node located at $\mathbf{x}_r \in \mathcal{A}$, the *local* channel gain (CG) map denoted by $g_{\mathbf{x} \rightarrow \mathbf{x}_r}(t, f)$ represents the CG of the link $\mathbf{x} \rightarrow \mathbf{x}_r$ for an arbitrary position $\mathbf{x} \in \mathcal{A}$, not necessarily occupied by a CR node. Similarly, for an *arbitrary* location $\mathbf{x}_s \in \mathcal{A}$, where none of the CRs resides, the *global* CG map collects the propagation coefficient of link $\mathbf{x} \rightarrow \mathbf{x}_s$ (Dall’Anese et al., 2011a); i.e., it contains CGs of links disjoint from any of the CR-to-CR links. Omitting the map’s dependence on f for brevity (as separate maps can be constructed for each f), the CG $g_{\mathbf{x} \rightarrow \mathbf{x}_s}(t)$ can be decomposed into path loss, shadowing and small-scale fading effects (Rappaport, 1996; Stüber, 2001). Averaging out small-scale fading (Goldsmith et al., 1994), one obtains

$$G_{\mathbf{x} \rightarrow \mathbf{x}_s}(t) := 10 \log_{10} g_{\mathbf{x} \rightarrow \mathbf{x}_s}(t) = G_0 - 10\alpha \log_{10}(\|\mathbf{x} - \mathbf{x}_s\|_2) + s_{\mathbf{x} \rightarrow \mathbf{x}_s}(t) \quad (11)$$

where G_0 denotes the path gain per unit distance, α the path loss exponent, and $s_{\mathbf{x} \rightarrow \mathbf{x}_s}(t)$ the shadow fading in dB at time t . Once G_0 and α are known, the CG map $g_{\mathbf{x} \rightarrow \mathbf{x}_s}(t)$ can be obtained provided the shadowing component

can be predicted for every pair of points $\mathbf{x}_s, \mathbf{x} \in \mathcal{A}$.

The steps in constructing CG maps are: 1) characterization of the correlation among channel coefficients over different wireless links; and 2) development of an appropriate statistical inference algorithm leveraging the channel correlation to predict propagation gains of arbitrary links.

1) *Spatio-temporal channel correlation*: The shadowing, created by attenuation and diffraction of propagating signals owing to obstructions, can be accurately modeled as log-normal distributed (Rappaport, 1996; Stüber, 2001); thus, Gaussian-distributed when expressed in dB. However, characterization of its correlation is challenging, especially when samples are taken at different locations and time instants. Well-established correlation models for shadow fading are available for cellular networks, in which mobile terminals are assumed to move with constant velocity (Gudmundson, 1991). An extension involving one mobile and two base stations was proposed in (Graziosi and Santucci, 2002), and multi-hop relay scenarios were studied in (Wang et al., 2006). An experimentally validated parametric model for nomadic as well as mobile distributed channels was reported in (Oestges et al., 2010). The importance of shadowing in analyzing performance of wireless ad hoc networks was pointed out in (Agrawal and Patwari, 2009), where a spatial correlation model was put forth to capture correlation of shadowing through a common “spatial loss” field $\ell(\mathbf{x}, t)$. Specifically, shadow fading is modeled as

$$s_{\mathbf{x} \rightarrow \mathbf{x}_s}(t) = \frac{1}{\|\mathbf{x} - \mathbf{x}_s\|_2^{1/2}} \int_{\mathbf{x}}^{\mathbf{x}_s} \ell(\mathbf{u}, t) d\mathbf{u}. \quad (12)$$

To allow spatio-temporal tracking of propagation gains, the spatial correlation model of (Agrawal and Patwari, 2009) was judiciously extended to accommodate temporal variations in (Dall’Anese et al., 2011a). In particular, inspired by spatio-temporal modeling approaches in geostatistics and environmental science (Mardia et al., 1998; Wikle and Cressie, 1999), the dynamics of the spatial loss field are captured as

$$\ell(\mathbf{x}, t) = \bar{\ell}(\mathbf{x}, t) + \tilde{\ell}(\mathbf{x}, t), \quad \text{and} \quad \bar{\ell}(\mathbf{x}, t) = \int_{\mathcal{A}} w(\mathbf{x}, \mathbf{u}) \bar{\ell}(\mathbf{u}, t-1) d\mathbf{u} + \eta(\mathbf{x}, t) \quad (13)$$

where $\bar{\ell}(\mathbf{x}, t)$ is spatially and temporally colored with $w(\mathbf{x}, \mathbf{u})$ modeling the interaction between $\ell(\mathbf{x}, t-1)$ at position \mathbf{x} at time t and $\ell(\mathbf{u}, t-1)$ at position \mathbf{u} at time $(t-1)$; and $\tilde{\ell}(\mathbf{x}, t)$ and $\eta(\mathbf{x}, t)$ are spatially colored yet temporally white zero-mean Gaussian stationary random fields. Plugging (13) into (12) yields $s_{\mathbf{x} \rightarrow \mathbf{x}_s}(t) = \bar{s}_{\mathbf{x} \rightarrow \mathbf{x}_s}(t) + \tilde{s}_{\mathbf{x} \rightarrow \mathbf{x}_s}(t)$, with the former spatially and temporally colored and the latter spatially colored but temporally white.

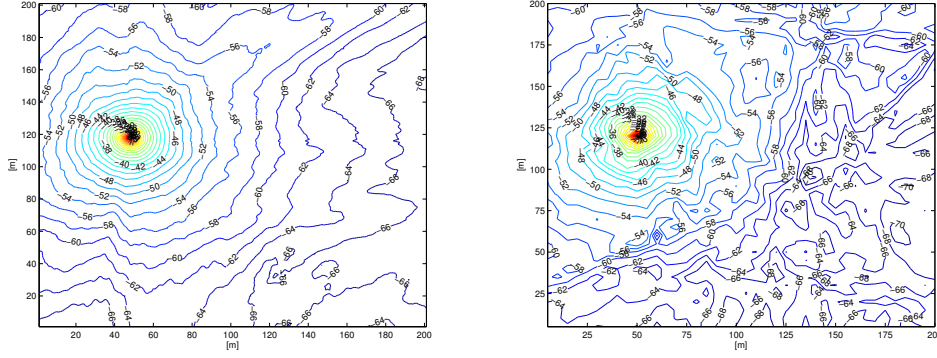
From a signal processing perspective, it would be desirable to reduce the dimensionality of the state-space model described by (13). One way to do it is through a basis expansion representation. Let $\{\psi_k(\cdot)\}_{k=1}^{\infty}$ be a set of complete prespecified orthonormal bases defined on \mathcal{A} . Then, $\bar{\ell}(\mathbf{x}, t)$ and $w(\mathbf{x}, \mathbf{u})$ can be approximated as $\bar{\ell}(\mathbf{x}, t) = \sum_{k=1}^K \chi_k(t) \psi_k(\mathbf{x})$ and $w(\mathbf{x}, \mathbf{u}) = \sum_{k=1}^K \beta_k(\mathbf{x}) \psi_k(\mathbf{u})$, where $\{\chi_k(t)\}$ and $\{\beta_k(\mathbf{x})\}$ are the basis expansion coefficients. Upon substituting these into (13), and sampling at locations $\{\mathbf{x}_r \in \mathcal{A}\}_{r=1}^{N_r}$, a finite-dimensional state equation for $\bar{\ell}(\mathbf{x}, t)$ is obtained as $\boldsymbol{\chi}(t) = \mathbf{T}\boldsymbol{\chi}(t-1) + \mathbf{J}\boldsymbol{\eta}(t)$ with $\boldsymbol{\chi}(t) := [\chi_1(t) \dots \chi_K(t)]^T$ denoting the state vector, and \mathbf{T} and \mathbf{J} determined from $\{\beta_k(\cdot)\}$ and $\{\psi(\cdot)\}$. This leads to a finite-dimensional representation of $\bar{s}_{\mathbf{x} \rightarrow \mathbf{x}_s}(t)$ as well. Specifically, upon defining $\phi_{\mathbf{x} \rightarrow \mathbf{x}_s, k} := (\|\mathbf{x}_s - \mathbf{x}\|)^{-1/2} \int_{\mathbf{x}_s}^{\mathbf{x}} \psi_k(\mathbf{u}) d\mathbf{u}$, $\bar{s}_{\mathbf{x} \rightarrow \mathbf{x}_s}(t)$ can be approximated as $\bar{s}_{\mathbf{x} \rightarrow \mathbf{x}_s}(t) \approx \boldsymbol{\phi}_{\mathbf{x} \rightarrow \mathbf{x}_s}^T \boldsymbol{\alpha}(t)$, where $\boldsymbol{\phi}_{\mathbf{x} \rightarrow \mathbf{x}_s} := [\phi_{\mathbf{x} \rightarrow \mathbf{x}_s, 1} \dots \phi_{\mathbf{x} \rightarrow \mathbf{x}_s, K}]^T$ depends only on the spatial coordinates \mathbf{x}_s and \mathbf{x} . Based on this spatio-temporal model for $s_{\mathbf{x} \rightarrow \mathbf{x}_s}(t)$, CG maps are constructed as follows.

2) *CG map construction*: Consider a network of N_r CRs $\{U_n\}_{n=1}^{N_r}$ at positions $\{\mathbf{x}_n\}_{n=1}^{N_r}$ known to one another, which exchange training signals in a time-division multiple-access (TDMA)-fashion to estimate their channel gains. Suppose that each CR U_n can measure the received powers from the transmissions of the set \mathcal{M}_n of nodes, where $\mathcal{M}_n \subset \{U_1, \dots, U_{N_r}\} \setminus \{U_n\}$. With node $U_j \in \mathcal{M}_n$ transmitting its training sequence over a given TDMA slot at time t , receiver U_n can estimate $g_{\mathbf{x}_j \rightarrow \mathbf{x}_n}(t)$ (and thus $G_{\mathbf{x}_j \rightarrow \mathbf{x}_n}(t)$ after translating it to a dB scale) by measuring the received power. Subtracting the known deterministic path loss from the path gain, a measurement $\check{s}_{\mathbf{x}_j \rightarrow \mathbf{x}_n}(t)$ of shadowing $s_{\mathbf{x}_j \rightarrow \mathbf{x}_n}(t)$ is readily obtained. Let $\check{\mathbf{s}}_n(t)$ denote the vector collecting $\{\check{s}_{\mathbf{x}_j \rightarrow \mathbf{x}_n}(t)\} \forall U_j \in \mathcal{M}_n$. Then, by pooling measurements from all CRs to a super-vector $\check{\mathbf{s}}(t) := [\check{\mathbf{s}}_1^T(t), \dots, \check{\mathbf{s}}_{N_r}^T(t)]^T$, one can write

$$\check{\mathbf{s}}(t) = \boldsymbol{\Phi} \boldsymbol{\alpha}(t) + \tilde{\mathbf{s}}(t) + \boldsymbol{\epsilon}(t) \quad (14)$$

where $\boldsymbol{\Phi}$ and $\tilde{\mathbf{s}}(t)$ are constructed with rows $\{\boldsymbol{\phi}_{\mathbf{x}_j \rightarrow \mathbf{x}_n}^T\}$ and entries $\{\check{s}_{\mathbf{x}_j \rightarrow \mathbf{x}_n}(t)\}$, $n = 1, \dots, N_r$, respectively; and $\boldsymbol{\epsilon}(t)$ captures Gaussian-distributed measurement errors (Goldsmith et al., 1994).

Based on the spatio-temporal model for $\bar{s}_{\mathbf{x} \rightarrow \mathbf{x}_s}(t)$, and the measurement equation (14), an adaptation of the Kriged Kalman filtering (KKF) to track the time-varying shadowing field was proposed in (Kim et al., 2011a; Dall'Anese et al., 2011a). KKF is a universal Kriging approach (Ripley, 1981), where the spatio-temporal evolution of $\bar{s}_{\mathbf{x} \rightarrow \mathbf{x}_s}$ is tracked via Kalman filtering (KF) (Mardia et al., 1998; Wikle and Cressie, 1999). Then, the shadow fading map $s_{\mathbf{x} \rightarrow \mathbf{x}_s}(t)$ is obtained $\forall \mathbf{x}_s, \mathbf{x}, t$ by complementing the trend estimate with an estimate of $\bar{s}_{\mathbf{x} \rightarrow \mathbf{x}_s}(t)$



(a) True map.

(b) Estimated map.

Fig. 6. Global CG map.

obtained via Kriging interpolation (Ripley, 1981). Specifically, let $\hat{\alpha}(t|t) := \mathbb{E}\{\alpha(t)|\check{\mathbf{s}}_{1:t}\}$ be the minimum mean-square error (MMSE) estimate of $\alpha(t)$ obtained via KF, given the accumulated data $\check{\mathbf{s}}_{1:t} := \{\check{\mathbf{s}}(\tau)\}_{\tau=1}^t$. Further, let $\mathbf{P}(t|t) := \text{cov}\{\alpha(t)|\check{\mathbf{s}}_{1:t}\}$ be the KF estimation error covariance matrix. Then, conditioned on $\check{\mathbf{s}}_{1:t}$, the shadow fading process $s_{\mathbf{x} \rightarrow \mathbf{x}_s}(t)$ for any $\mathbf{x}_s, \mathbf{x} \in \mathcal{A}$, is Gaussian distributed with mean and variance given, respectively, by

$$\hat{s}_{\mathbf{x} \rightarrow \mathbf{x}_s}(t) := \mathbb{E}\{s_{\mathbf{x} \rightarrow \mathbf{x}_s}(t)|\check{\mathbf{s}}_{1:t}\} = \boldsymbol{\phi}_{\mathbf{x} \rightarrow \mathbf{x}_s}^T \hat{\alpha}(t|t) + \mathbf{c}_{\check{\mathbf{s}}}^T(\mathbf{x}_s, \mathbf{x}) \boldsymbol{\Sigma}^{-1} [\check{\mathbf{s}}(t) - \boldsymbol{\Phi} \hat{\alpha}(t|t)] \quad (15a)$$

$$\begin{aligned} \sigma_{\mathbf{x} \rightarrow \mathbf{x}_s}^2(t) := \text{var}\{s_{\mathbf{x} \rightarrow \mathbf{x}_s}(t)|\check{\mathbf{s}}_{1:t}\} &= \sigma_{\check{\mathbf{s}}}^2 - \mathbf{c}_{\check{\mathbf{s}}}^T(\mathbf{x}_s, \mathbf{x}) \boldsymbol{\Sigma}^{-1} \mathbf{c}_{\check{\mathbf{s}}}(\mathbf{x}_s, \mathbf{x}) \\ &+ [\boldsymbol{\phi}_{\mathbf{x} \rightarrow \mathbf{x}_s}^T - \mathbf{c}_{\check{\mathbf{s}}}^T(\mathbf{x}_s, \mathbf{x}) \boldsymbol{\Sigma}^{-1} \boldsymbol{\Phi}] \mathbf{P}(t|t) [\boldsymbol{\phi}_{\mathbf{x} \rightarrow \mathbf{x}_s} - \boldsymbol{\Phi}^T \boldsymbol{\Sigma}^{-1} \mathbf{c}_{\check{\mathbf{s}}}(\mathbf{x}_s, \mathbf{x})] \end{aligned} \quad (15b)$$

where $\mathbf{c}_{\check{\mathbf{s}}}(\mathbf{x}_s, \mathbf{x}) := \mathbb{E}\{\check{\mathbf{s}}(t) \tilde{s}_{\mathbf{x} \rightarrow \mathbf{x}_s}(t)\}$, and $\boldsymbol{\Sigma} := \text{cov}\{\check{\mathbf{s}}(t)\} + \text{cov}\{\epsilon(t)\}$. The CG map estimate $\hat{G}_{\mathbf{x} \rightarrow \mathbf{x}_s}(t)$ can now be constructed from $\hat{s}_{\mathbf{x} \rightarrow \mathbf{x}_s}(t)$ by adding back the deterministic path loss component; i.e., $\hat{G}_{\mathbf{x} \rightarrow \mathbf{x}_s}(t) = G_0 - 10\alpha \log_{10}(\|\mathbf{x} - \mathbf{x}_s\|_2) + \hat{s}_{\mathbf{x} \rightarrow \mathbf{x}_s}(t)$. Means of acquiring \mathbf{T} , $\mathbf{c}_{\check{\mathbf{s}}}$ and $\boldsymbol{\Sigma}$ can be found in (Kim et al., 2011a).

Fig. 6(a) shows the (true) CG map corresponding to a PU located at $\mathbf{x}_s = (50, 120)$ m. Path loss parameters are set to $G_0 = 0$ and $\alpha = 3$. Clearly, the CG map exhibits a peak at location \mathbf{x}_s ; however, due to the spatially inhomogeneous shadowing component $s_{\mathbf{x} \rightarrow \mathbf{x}_s}(t)$, whose standard deviation is approximately 10 dB, the overall CG map decays non-isotropically. Thus, estimating the shadowing field is essential for CR network operation and effective PU protection. To estimate the CG map, 20 CRs uniformly distributed over a square area of 200 m \times 200 m exchange signals to acquire propagation gains; the communication range was set to 125 m. An estimated version of the map in Fig. 6(a) is depicted in Fig. 6(b). It can be seen that the KKF-based spatial interpolation can

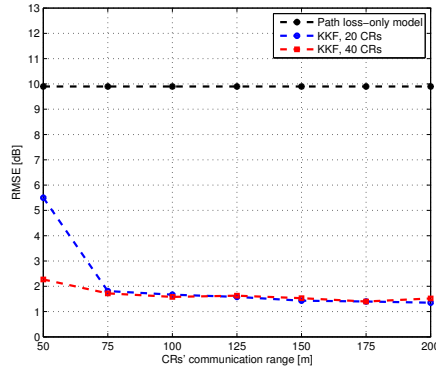


Fig. 7. Standard deviation of CG map estimation error.

effectively predict the shadow fading process (and hence the channel gains) even in locations where no measurements were made. The error in reconstructing the map, evaluated over a grid of 36 evenly spaced locations was 1.5 dB, significantly lower than the standard deviation of the shadow fading. Fig. 7 depicts the root-mean-square-errors (RMSEs) of the KKF for variable communication range and number of collaborating CRs. One can notice that the map estimation quality is maintained even when connectivity of the CR network is sparse due to shorter communication ranges.

3) *Coverage region estimation*: Although sensing schemes can locate active PUs, particularly challenging is to acquire the locations of “passive” PUs, which do not transmit but just listen. Nonetheless, those receivers still need to be protected from interference under the PU-CR hierarchy (Zhao and Sadler, 2007). To this end, the coverage region of the PUs can be computed, where *potential* PU receivers can reside. This illustrates an application of the CG maps.

Let $\Pi_{\mathbf{x}}(t)$ denote the average power in dB received at location $\mathbf{x} \in \mathcal{A}$ due to the transmission of a PU located in \mathbf{x}_s signaling at power $P_s := 10 \log_{10} p_s$. Then, $\Pi_{\mathbf{x}}(t)$ can be expressed as $\Pi_{\mathbf{x}}(t) = P_s + G_0 - 10\alpha \log_{10} \|\mathbf{x}_s - \mathbf{x}\|_2 + s_{\mathbf{x} \rightarrow \mathbf{x}_s}(t)$. Based on the estimated CG map, $\Pi_{\mathbf{x}}(t)$ can be modeled as Gaussian distributed with mean $P_s + G_0 - 10\alpha \log_{10} \|\mathbf{x}_s - \mathbf{x}\|_2 + \hat{s}_{\mathbf{x} \rightarrow \mathbf{x}_s}(t)$ and variance $\sigma_{\mathbf{x} \rightarrow \mathbf{x}_s}^2(t)$.

Since a PU receiver can reliably decode the desired message only if the received power exceeds a certain threshold Π_{\min} (dB), one can compute the probability that a PU receiver at \mathbf{x} can decode as (Goldsmith, 2005, Ch. 2)

$$P_{\mathbf{x}}^{cov}(t) := \Pr\{\Pi_{\mathbf{x}}(t) \geq \Pi_{\min}\} = Q\left(\frac{\Pi_{\min} - P_s - G_0 + 10\alpha \log_{10} \|\mathbf{x}_s - \mathbf{x}\|_2 - \hat{s}_{\mathbf{x} \rightarrow \mathbf{x}_s}(t)}{\sigma_{\mathbf{x} \rightarrow \mathbf{x}_s}(t)}\right) \quad (16)$$

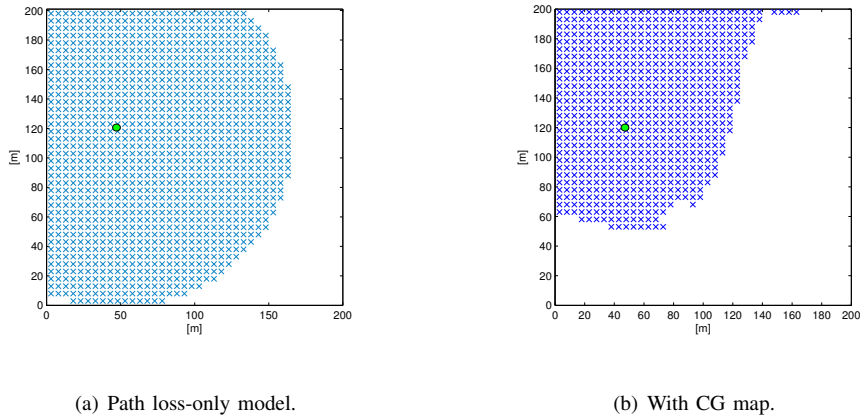


Fig. 8. Coverage region of a PU transmitter.

where $Q(\cdot)$ is the standard Gaussian tail function. The coverage region of the device located in \mathbf{x}_s is defined as the set of locations in \mathcal{A} , for which the coverage probability is no smaller than a threshold ν (Goldsmith, 2005, Ch. 2); i.e., $\mathcal{C}(t) := \{\mathbf{x} \in \mathcal{A} | P_{\mathbf{x}}^{cov}(t) \geq \nu\}$. In the absence of CG map knowledge, CRs would set $\hat{s}_{\mathbf{x}_s \rightarrow \mathbf{x}}(t) = 0$; consequently, \mathcal{C} would reduce to a time-invariant disc centered at \mathbf{x}_s ; see Fig. 8(a) with $\Pi_{\min} = -60$ dB and $\nu = 0.4$. On the contrary, the CG map can portray the coverage region more accurately as depicted in Fig. 6(b). The approach can also accommodate small-scale fading effects, as the composite log-normal and Nakagami fading turns out to be well approximated as log-normal (Hong et al., 2008; Dall’Anese et al., 2011b).

III. SENSING AT THE MAC LAYER

Spectrum sensing at the PHY layer is primarily concerned with detection of PU signals for the purpose of identifying transmission opportunities and creating spatio-temporal RF maps. In practice however, the PU spectrum is several times wider than the sensing bandwidth of a single CR transceiver. The *goal* of MAC layer sensing is to *schedule* the sensing operations of CRs across bands so as to locate maximal transmission opportunities. The MAC layer sensing problem is not trivial, as it involves balancing resources between sensing and communication. If multiple CRs are present, the MAC sensing algorithm must also take into account the possible contention among the CRs for medium access.

The design of MAC sensing algorithms is guided mainly by the rate at which the underlying spectrum occupancy changes. Slow temporal variations in the spectrum occupancy, as encountered in the TV bands, allow for longer sensing intervals. Consequently, MAC sensing algorithms in these bands simply search exhaustively through a

wide range of frequencies before transmitting. On the other hand, fast spectral variations, as in the cellular bands, allow for only a few bands to be sensed before transmission. Therefore, the MAC sensing algorithms here need to utilize statistical inference to predict spectrum occupancy in order to better schedule sensing operations across bands. An alternative approach would be to design the analog front end of the CRs suitable for wideband spectrum sensing (Blaschke et al., 2008). In this case, the trade-off between the complexity of the sensing hardware including the analog-to-digital converters (ADCs) and the sensing accuracy must be carefully examined (Le et al., 2005). In the sequel, the focus will be on the MAC sensing algorithms based on low-complexity narrowband sensing hardware.

A. *Wireless regional area networks*

The IEEE 802.22 standard for wireless regional area networks (WRAN) specifies a MAC sensing protocol for CRs operating on the spectrum assigned to TV services (between 47-910 MHz) (Cordeiro et al., 2005). The sensing in IEEE 802.22 operates in two stages: a *fast sensing* stage involving rapid probes on multiple bands, each lasting at most a millisecond; and a *fine sensing* stage lasting 25 milliseconds, on a specific band determined by the outcome of the first stage. The MAC layer also schedules *in-band* sensing for determining if a PU starts transmitting before active CRs have completed their transmissions. Distributed sensing is enabled by scheduling periodic *quiet times* (during which all CRs must stop their transmissions in order to sense) and exchange of band occupancy reports among CRs.

Since the presence of periodic quiet times interrupts CR transmissions, an alternative dynamic frequency hopping mode has been proposed for CRs with multiple transceivers (Hu et al., 2007). In this mode, a sensing transceiver is used to identify out-of-band opportunities *while* concurrent CR transmission, thus eliminating the need for quiet times. Related works have dealt with other practical issues pertaining to the coexistence of multiple CR networks, presence of hidden PU nodes (Sengupta et al., 2007), and co-channel interference in multi-cell environments (Willkomm et al., 2008).

B. *Cellular networks: MAC sensing as an inference problem*

As mentioned earlier, the two-stage sensing operation for WRANs is not feasible in cellular systems, where band occupancy varies far more quickly. MAC sensing algorithms in this case employ statistical inference methods by

utilizing the observed history of spectrum occupancy. The first step for MAC sensing involves band occupancy prediction using time-series models, and is described in the next subsection.

1) *Band occupancy prediction*: A binary time-series prediction approach has been proposed in (Yarkan and Arslan, 2007). Consider a synchronous time-slotted PU network operating over N licensed bands. The PU network state at the MAC layer can be specified by an $N \times 1$ vector $\mathbf{s}(t)$ with entries $s_n(t) \in \{0(\text{occupied}), 1(\text{idle})\}$, $n = 1, \dots, N$. Given p samples $\mathbf{s}(t-p), \dots, \mathbf{s}(t-1)$, logistic regression is used to predict the probability of band occupancy at time t , i.e.,

$$\Pr(s_n(t) = 1) = \frac{1}{1 + \exp(-(a_{n0} + \sum_{j=1}^p a_{nj}s_n(t-j) + v_n(t)))} \quad 1 \leq n \leq N \quad (17)$$

with regression coefficients $\{a_{nj}\}_{j=0}^p$, intercepts (or offsets) a_{n0} , and noise term $v_n(t)$ for $n = 1, \dots, N$. The coefficients $\{a_{nj}\}_{j=0}^p$ may be estimated by taking M observations per band, and maximizing the log-likelihood function (Bishop, 2006)

$$\hat{\mathbf{a}}_n = \arg \max_{\mathbf{a}_n} \sum_{m=p+1}^M s_{nm} \log q_{nm}(\mathbf{a}_n) + (1 - s_{nm}) \log(1 - q_{nm}(\mathbf{a}_n)) \quad 1 \leq n \leq N \quad (18)$$

where \mathbf{a}_n stacks the terms $\{a_{nj}\}_{j=0}^p$, and $q_{nm}(\mathbf{a}_n) := 1/[1 + \exp(-a_{n0} - \sum_{j=1}^p a_{nj}s_n(m-j))]$.

An alternative approach in this context is described in (Li and Zekavat, 2008), that utilizes nonstationary autoregressive time-series models. In this framework, PU packet arrivals (and subsequently the number of PU transmissions) for each band follow a non-homogeneous Poisson process $\{\mathcal{A}(t), t \geq 0\}$ with time-varying rate parameter $\lambda(t)$. Packet arrivals within a time slot $(t, t+T_s)$ may then be modeled by a Poisson process with constant rate λ_ℓ/T_s , where $\lambda_\ell := \int_{t=\ell T_s}^{(\ell+1)T_s} \lambda(t) dt$. A seasonal autoregressive integrated moving average (SARIMA) model is proposed in (Li and Zekavat, 2008) to track the rates $\{\lambda_\ell\}$, which takes the form

$$\lambda_\ell = \lambda_{\ell-1} + \lambda_{\ell-24} - \lambda_{\ell-25} + z_\ell + \theta z_{\ell-1} + \Theta z_{\ell-24} + \theta \Theta z_{\ell-25} \quad (19)$$

where $T_s = 1$ hour, and $z_\ell \sim \mathcal{N}(0, \sigma^2)$ is an error term. The model parameters $(\theta, \Theta, \sigma^2)$ are estimated using techniques described in (Brockwell and Davis, 2006). In contrast to the logistic regression approach of (Yarkan and Arslan, 2007), SARIMA models allow nonparametric approaches for prediction of band occupancies, and handle trend and seasonal nonstationarities.

In a nutshell, high-order time-series models enable prediction of spectrum occupancies, and can be utilized for scheduling sensing operations across bands. However, since prediction must be carried out per band, these models

become highly inefficient in terms of sensing overload and computational complexity if the number of available bands is large. The next section details joint prediction and scheduling MAC sensing algorithms that scale gracefully with the number of available bands.

2) *Band occupancy scheduling*: Since sensing is performed only on a fraction of available bands, the algorithms described in this section perform prediction based only on the observed spectrum occupancy history. One of the early MAC sensing algorithms in this context was proposed in (Zhao et al., 2007), where evolution of the PU state $\mathbf{s}(t)$ is assumed to follow a Markov chain with known transition probabilities $p_{ij} := P(\mathbf{s}(t) = \mathbf{i} | \mathbf{s}(t-1) = \mathbf{j})$, for all $\mathbf{i}, \mathbf{j} \in \{0, 1\}^{2^N}$, that stay constant for at least T time slots, and can be estimated as described in (Long et al., 2008). Each CR seeks to access the spectrum opportunities that arise when one or more of the bands are idle. Owing to hardware constraints, a CR can only sense at most $L_1 \leq N$ bands, and access at most $L_2 \leq L_1$ bands. Consequently, at time slot t , the CR chooses a subset $\mathcal{B}_s(t)$ (with cardinality not exceeding L_1) of bands to sense, and a subset $\mathcal{B}_a(t) \subseteq \mathcal{B}_s(t)$ of bands to access, thus achieving a throughput of

$$R_{\{\mathcal{B}_s(t), \mathcal{B}_a(t)\}}(t) := \sum_{n \in \mathcal{B}_a(t)} s_n(t) \beta_n \quad (20)$$

where β_n is the bandwidth of the n -th band. The goal is to sequentially choose $\mathcal{B}_s(t)$ and $\mathcal{B}_a(t)$ to maximize the total throughput achieved in T time slots, averaged over all possible state vectors $\{s_n(t)\}$.

Since the network state is not directly observable by the CRs, beliefs $\lambda_i(t) := \Pr(\mathbf{s}(t) = \mathbf{i} | \mathcal{H}(t))$ are utilized to make the sensing and access decisions, using the observed spectrum availability history $\mathcal{H}(t) := \{s_n(\ell) \forall n \in \mathcal{B}_s(\ell), 1 \leq \ell \leq t-1\}$. Collecting the beliefs in $\boldsymbol{\lambda}(t)$, a policy is defined as the function $\pi(t) : \boldsymbol{\lambda}(t) \rightarrow \{\mathcal{B}_s(t), \mathcal{B}_a(t)\}$.

The optimal policy is given by

$$\{\pi^*(t)\}_{t=1}^T = \arg \max_{\{\pi(t)\}_{t=1}^T} \mathbb{E} \left[\sum_{t=1}^T R_{\{\mathcal{B}_s(t), \mathcal{B}_a(t)\}}(t) | \mathcal{H}(1) \right]. \quad (21)$$

The problem of determining the optimal policy can now be solved using a partially observable Markov decision process (POMDP) framework, as detailed in (Zhao et al., 2007). Note however that the size of the state space of (21) is exponential in N , which makes this approach inefficient for a large number of bands. The state space and hence the problem size can be reduced to N if the bands are assumed to evolve independently. The independence assumption decouples the problem into N sub-problems, each with a two-state Markov chain as shown in (Zhao et al., 2007; Zhao and Swami, 2007). The case of independently evolving bands can also be related to the restless multi-armed

bandit problem (Liu and Zhao, 2010), which allows for sensing algorithms with even lower complexity. Further works have extended the approach to include energy constraints (Hoang et al., 2009), and sensing imperfections (Chen et al., 2008). To address the exponential complexity of the general POMDP approach, the impact of using myopic policies is examined in (Zhao et al., 2008b). These policies only maximize the expected throughput over the next time slot, but are still optimal under certain conditions.

A similar problem is considered in (Unnikrishnan and Veeravalli, 2010), but a separate control channel is allowed for each CR. The control channel is shown to enable better synchronization, alleviation of the hidden node problem, and consequently improved spectrum utilization. A hardware constrained MAC design is pursued in (Jia et al., 2008), which optimizes the sensing time while respecting hardware constraints such as single transceiver, partial spectrum sensing and limited spectrum aggregation. The intuition is that sensing for longer periods uncovers more suitable bands but leaves little time for communication. The optimal stopping time is derived by employing a dynamic programming approach; a related example is described in detail in the context of cross-layer sensing in Sec. IV-A1. Extending the approach to consider heterogeneous bands with varying capacities, the problem of determining the optimal sensing order is investigated in (Cheng and Zhuang, 2011).

In an attempt to relax the time-slotted assumption in (Zhao et al., 2007) and related works, a continuous-time Markov chain approach has been proposed for modeling the band occupancy process (Geirhofer et al., 2007). In this case, the state is defined similarly as before, but a band stays in state i (busy/idle) for an exponentially distributed time period (with rate λ_i or μ_i). The sensing operation may then be viewed as sampling the state process $\mathbf{s}(t)$ in a periodic fashion. Specifically, the N bands are sensed in a round-robin fashion, with exactly one sample per time slot (of duration T_s). After each sensing operation, the MAC layer schedules a transmission on a selected band. It is shown in (Zhao et al., 2008a) that periodic sampling yields a discrete time Markov chain of sampled state vectors, whose transition probabilities can be derived in closed form. This allows for the transmission scheduling problem to be cast within the POMDP framework, yielding an optimal medium access policy. The framework also allows for the inclusion of constraints on the collision probabilities in a straightforward way (Li et al., 2011). A more general semi-Markov model has also been proposed, where the busy/idle times have arbitrary distributions $f_i^1(x)$ and $f_i^0(x)$ (Kim and Shin, 2008a). Related problems include the choice of sensing period (Kim and Shin, 2008a), sensing order (Kim and Shin, 2008b), and more generally the sensing policy in time and frequency (Huang et al.,

2009). Finally, the sensing order and optimal sensing policy design for the multiuser scenario have been considered in (Fan and Jiang, 2009; Lai et al., 2011).

IV. CR SENSING AND CROSS-LAYER DESIGN

As is the case with most PHY/MAC functions in wireless communication systems, spectrum sensing is not an isolated task that can be designed independently of other components in the CR system. It is important when designing sensing algorithms to also take into account the overall system objectives. Further, given the enhanced awareness of the RF environment in which the CRs operate, it is essential to adapt the higher-layer tasks to the environment to maximize efficiency and the overall CR network performance.

As was mentioned in Sec. III, there is a trade-off between sensing accuracy and network-wide performance objectives such as throughput, delay, and reliability. Consider for example the trade-off between sensing duration and throughput. As was explained in Sec. II, the basic element of the sensing device is the detector that discriminates the H_1 hypothesis that says there is an ongoing PU transmission, from the H_0 hypothesis that says the spectrum is unoccupied. Since the sensing is done typically in challenging situations such as at a low SNR and without explicit support from the PU systems, typically a large number of samples must be collected for reliable detection. This inevitably increases sensing time. On the other hand, only when the sensing is finished (and the medium is determined to be idle), can the CR proceed to actual data transmission. Therefore, given that the total idle duration is limited (as the PU can come back and transmit), the more time is devoted to sensing, the less time is left for useful data transmission. Such a trade-off was studied in detail in (Liang et al., 2008) for fixed sample size (FSS) test-based sensing. A similar trade-off was investigated in the context of MAC layer design of sensing algorithms in (Jia et al., 2008; Jiang et al., 2009).

Even when the sensing duration is fixed, there is trade-off between the probability of miss detection and the probability of false alarm, which affects the system objectives. To see this, one needs to note that if the detector misses the presence of PUs, it is likely that the CR will proceed to data transmission, causing interference to the licensed users. Thus, a low miss detection probability is desired, which in turn increases the false alarm probability. However, the false alarms result in wasted opportunities for CR transmission, thus reducing system efficiency. This problem becomes only more interesting when multiple bands must be sensed concurrently, as was explored in (Quan

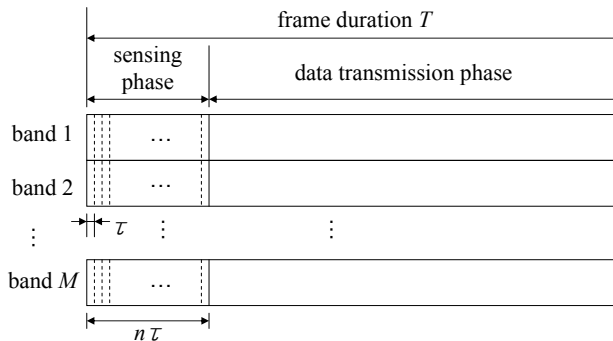


Fig. 9. CR frame structure.

et al., 2009; Zhao and Ye, 2008; Fan and Jiang, 2010); see also (Kundargi and Tewfik, 2007; Kim and Giannakis, 2009; Xin et al., 2009; Kim and Giannakis, 2010; Kim et al., 2011b) for sequential alternatives in this context. Some of these formulations will be reviewed in Sec. IV-A.

An equally important issue is how to effectively tap into the significantly improved awareness of the RF environment obtained through the sensing and the RF cartography, for design and operation of higher-layer networking protocols. Numerous challenges in this direction include distributed resource optimization, quality-of-service management, and maintaining network robustness under uncertainty (Cheng et al., 2007; Shi and Hou, 2008; Shiang and van der Schaar, 2009). In Sec. IV-B, a recently developed robust routing scheme exploiting the RF maps will be showcased.

A. Joint Sensing and Resource Optimization

While the FSS test-based sensing algorithms must fix the number of samples used for detection before actually “seeing” those samples, the sequential alternatives can decide on the fly whether the samples collected so far are informative enough for reliable detection, and continue taking samples if not. For a binary hypothesis testing problem, sequential probability ratio test (SPRT) is a well-established algorithm that minimizes the sample size on the average, for given detection and false alarm probability specifications. It can be applied in a straightforward manner to the single-band sensing problem as outlined in Sec. II. A low complexity alternative based on energy detection was analyzed in (Xin et al., 2009). Next, the more challenging case of multi-band joint sensing is reviewed using the sequential detection approaches.

1) *Throughput-aware sequential sensing*: Consider a CR receiver that scans M bands in parallel for transmission opportunities. Due to self-interference issues, the radio is assumed to be half-duplex; i.e., it cannot sense on one band while transmitting on another. Thus, a CR frame of duration T is divided into a sensing phase of duration $n\tau$ (where τ is the sampling interval) and a data transmission phase of duration $(T - n\tau)$; see Fig. 9.

Under the assumption that the spectrum occupancy of the PUs is independent across bands, binary hypothesis tests need to be performed on each band $m \in \{1, 2, \dots, M\}$. Denoting the samples obtained at time n as $\{r_n^{(m)}\}$, one aims to discriminate the following two hypotheses for band m .

$$\begin{aligned} H_0^{(m)} : r_n^{(m)} &= z_n^{(m)}, \quad n \in \{1, \dots, N\} \\ H_1^{(m)} : r_n^{(m)} &= h_n^{(m)} s_n^{(m)} + z_n^{(m)}, \quad n \in \{1, \dots, N\} \end{aligned} \quad (22)$$

where $\{h_n^{(m)}\}$ denote the channel coefficients, and $\{z_n^{(m)}\}$ the noise. Adopting energy detection, the observation at time n is defined as $y_n^{(m)} := |r_n^{(m)}|^2$.

Let $\delta_n^{(m)} \in \{1, 0\}$ denote the permit-to-access decision for channel m , made after seeing up to the n -th sample; if it is equal to 1, the channel is deemed idle (i.e., $H_0^{(m)}$ in effect), and 0 otherwise. Define $\boldsymbol{\delta}_n := [\delta_n^{(1)} \delta_n^{(2)} \dots \delta_n^{(M)}]^T$. Denote also the PU occupancy over the M channels by \mathcal{H} , whose m -th entry $\mathcal{H}^{(m)}$ takes values from $\{H_0^{(m)}, H_1^{(m)}\}$. We wish to characterize the effective throughput that the CR can enjoy. Let $R^{(m)}$ denote the known rate that can be achieved when transmitting over channel m . Then, if the CR stops sensing after n sampling intervals and proceeds to data transmission, the overall throughput can be written as ($\mathbb{1}_{\{\cdot\}}$ denotes the indicator function)

$$f'_n(\mathcal{H}, \boldsymbol{\delta}_n) = \frac{T - n\tau}{T} \sum_{m=1}^M R^{(m)} \mathbb{1}_{\{H_0^{(m)}\}} \delta_n^{(m)}, \quad n = 1, 2, \dots, N, \quad N\tau \leq T. \quad (23)$$

From (23), the throughput-sensing trade-off is apparent: as the number of observed samples increases, the factor $\frac{T-n\tau}{T}$ diminishes, but more available bands may be correctly identified to yield a higher value for the sum rate in (23).

Given the past observations $\mathbf{Y}_n \triangleq [\mathbf{y}_1 \mathbf{y}_2 \dots \mathbf{y}_n]$, the goal is to obtain the average throughput-optimal *stopping policy* $\Delta_n(\mathbf{Y}_n) \in \{S, \bar{S}\}$ that determines whether to stop (“ S ”) or not stop (“ \bar{S} ”) at each time n , and the *access policy* $\boldsymbol{\delta}_n(\mathbf{Y}_n) \in \{1, 0\}^M$ indicating whether each band may be used for data transmission if the sensing stops at

time n . In other words, the objective is to maximize the average throughput

$$E_{\mathbf{Y}_N, \mathcal{H}} \left\{ \sum_{n=1}^N \mathbb{1}_{\{\Delta_{n-1}=\bar{S}, \Delta_n=S\}} f'_n(\mathcal{H}, \delta_n) \right\} \quad (24)$$

over the control policies $\{\Delta_n(\cdot)\}_{n=1}^{N-1}$ and $\{\delta_n(\cdot)\}_{n=1}^N$. Here, $\mathbf{\Delta}_{n-1} := [\Delta_0 \ \Delta_1 \ \dots \ \Delta_{n-1}]$ with $\Delta_0 \equiv \bar{S}$, and $\mathbf{\Delta}_{n-1} = \bar{S}$ is a shorthand for $\Delta_0 = \Delta_1 = \dots = \Delta_{n-1} = \bar{S}$. Note also that $\Delta_N \equiv S$ by design, as we are dealing with a finite horizon problem. The indicator function in (24) ensures that the reward $f'_n(\cdot)$ is evaluated only at the smallest time slot n^* satisfying $\Delta_{n^*} = S$; for the rest of the time steps, $n < n^*$ and $n > n^*$, the summands are zero.

On the other hand, the CR access policy must ensure a low probability of “collision” with the ongoing PU transmissions due to miss detection. The “collision” probability $P_c^{(m)}$ on band m can be written as

$$P_c^{(m)} = \sum_{n=1}^N \Pr \left\{ \mathbf{\Delta}_{n-1} = \bar{S}, \Delta_n = S, \delta_n^{(m)} = 1 | H_1^{(m)} \right\} \quad (25)$$

which must be kept small; i.e. $P_c^{(m)} \leq \bar{\beta}$ for all m with $\bar{\beta}$ being a small positive threshold. Upon defining the so-called belief vector $\boldsymbol{\pi}_n := [\pi_n^{(1)} \ \dots \ \pi_n^{(M)}]^T$ with entries $\pi_n^{(m)} := \Pr \left\{ H_0^{(m)} | y_1^{(m)}, \dots, y_n^{(m)} \right\}$, one can show that $P_c^{(m)}$ can be equivalently expressed as (Kim and Giannakis, 2010)

$$P_c^{(m)} = E_{\mathbf{Y}_N} \left\{ \sum_{n=1}^N \mathbb{1}_{\{\Delta_{n-1}=\bar{S}, \Delta_n=S\}} \delta_n^{(m)} \frac{1 - \pi_n^{(m)}}{1 - \pi_0^{(m)}} \right\}. \quad (26)$$

Furthermore, by first taking conditional expectation given \mathbf{Y}_N , and then taking unconditioned expectation, the average throughput in (24) can also be written as

$$E_{\mathbf{Y}_N} \left\{ \sum_{n=1}^N \mathbb{1}_{\{\Delta_{n-1}=\bar{S}, \Delta_n=S\}} \frac{T - n\tau}{T} \sum_{m=1}^M R^{(m)} \pi_n^{(m)} \delta_n^{(m)} \right\}. \quad (27)$$

It can be verified that maximizing (27) over $\{\Delta_n(\cdot)\}_{n=1}^{N-1}$ and $\{\delta_n(\cdot)\}_{n=1}^N$ subject to $P_c^{(m)} \leq \bar{\beta}$ for all m adheres to the constrained dynamic programming (DP) formalism (Bertsekas, 2000). The problem can be tackled using Lagrange relaxation (non, 1997). Interestingly, the optimal permit-to-access policy $\delta_n^{*(m)}$ for each band m is found to be a likelihood ratio test with the threshold depending on the Lagrange multiplier associated with the band (Kim and Giannakis, 2010). A reduced-complexity, basis regression-based suboptimal stopping policy was also derived. It was seen that these policies could achieve a significant portion of the genie-aided policy (which non-causally possesses the information from the future observations), while significantly outperforming suboptimal 1-step look-ahead as well as the best FSS sensing schemes; see Fig. 10.

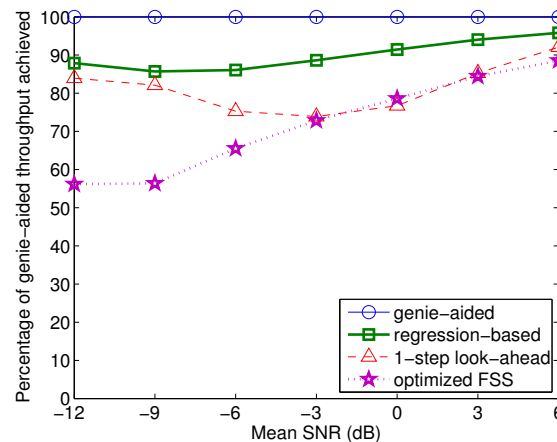


Fig. 10. Ratio of achieved average throughput relative to the genie-aided throughput.

2) *Sequential sensing for real-time traffic*: Another interesting challenge is to transport real-time traffic such as voice or video using CR networks. Real-time traffic often has stringent delay and minimum rate constraints. Thus, efficient design of the sensing algorithm is extremely important in this scenario. As a concrete paradigm, consider again the multi-band CR sensing problem, but with an outage constraint on the requested minimum rate. Thus, the goal is to minimize the sensing delay while finding enough number of idle bands that can support the given minimum rate with high probability.

Since the DP-based approach may be intractable with the chance constraint, a more structured approach was taken in (Kim et al., 2011b). Specifically, rather than formulating a rigorous DP problem to obtain the optimal access and stopping policies, a bank of SPRTs were used (one for each band) to sense the M bands in parallel. Then, an optimization problem was formulated to solve for the thresholds of the SPRTs to minimize the average sensing time while abiding by the minimum rate and the PU interference constraints. An important catch in this approach is that the stopping times of the individual SPRTs may be different. To mitigate this issue, a tractable objective of minimizing the largest average sensing time over the bands was employed. To much practical appeal, the associated optimization problem turns out to be convex (Kim et al., 2011b).

B. Cartography-Enabled Route Optimization

Volatile wireless connectivity in CR scenarios can be robustified via optimizing network operations leveraging spectrum sensing. Routing protocols for wireless networking hinge on the notion of network connectivity graph

to find source-to-destination paths optimal in some sense (Couto et al., 2003). The edge weights in CR network graphs should reflect spatio-temporal PU spectrum occupancy statistics, network-wide spectral opportunities, and propagation medium characteristics. Appropriate cross-layer design based on such information is instrumental for efficient resource allocation and for addressing end-to-end quality-of-service demands.

Based on the output of the sensing task, link weights can be used to indicate the amount of spectral resources available per CR-to-CR link (Xin et al., 2008). Optimal source-to-destination paths can then be found via Dijkstra or Bellman Ford algorithms. A two-phase approach combining static mesh routing with per-packet dynamic routing is proposed in (Pefkianakis et al., 2008), where network nodes first compute an expected route cost as well as a set of candidate forwarding nodes, and then route packets via links with highest channel quality. In (Abbagnale and Cuomo, 2010), a routing scheme is developed to avoid network zones with no guarantees of stable CR connectivity based on spatio-temporal statistics of the PU activities. The concept of coverage map is leveraged in (Chowdhury and Akyildiz, 2011) to devise routing strategies supporting multiple classes of routes, and hence different CR quality-of-service demands. The effects of random PU interference on CR links is accounted for in (Khalife et al., 2010), where the predicted capacity of each CR-to-CR link is exploited to compute the path that is most likely to meet CR end-to-end requirements. An optimal cross-layer design problem was considered in (Dall’Anese and Giannakis, 2012) to compute not only optimal routes, but also physical and medium access parameters that dictate the expected packet forwarding capabilities. In doing so, the statistics of propagation channels were exploited, along with PU state information provided by spectrum sensing.

Following (Dall’Anese and Giannakis, 2012), consider a CR wireless network sharing spectral resources with an incumbent PU system in an underlay setup (Zhao and Sadler, 2007) to route data packets to a sink node U_{N_r+1} . The dynamical and stochastic nature of the propagation medium naturally suggests stochastic routing strategies (Ribeiro et al., 2007, 2008), in which each CR node U_n decides per time slot whether to route packets toward a neighboring node U_i with probability $t_{\mathbf{x}_n \rightarrow \mathbf{x}_i} \in [0, 1]$. To capture channel- and interference-induced uncertainty, let $r_{\mathbf{x}_n \rightarrow \mathbf{x}_i} \in [0, 1]$ denote the probability that a packet transmitted from CR U_n is correctly decoded by U_i . As a result, the stochastic nature of data transport is captured by the pairwise packet delivery probabilities $\{t_{\mathbf{x}_n \rightarrow \mathbf{x}_i} r_{\mathbf{x}_n \rightarrow \mathbf{x}_i}\}$.

A well-established criterion for successful packet reception is to require the signal-to-interference-plus-noise ratio

(SINR) to stay above a certain threshold (Haenggi, 2005), which is determined by the receiver structure, transmit-power, modulation, and coding scheme. Recall that $g_{\mathbf{x}_n \rightarrow \mathbf{x}_i}$ denotes the log-normal-distributed propagation gain between U_n and U_i , which accounts for both shadowing and Nakagami fading (Hong et al., 2008; Stüber, 2001). Then, the SINR of link $\mathbf{x}_n \rightarrow \mathbf{x}_i$ can be expressed as

$$\gamma_{\mathbf{x}_n \rightarrow \mathbf{x}_i} := \frac{p_n g_{\mathbf{x}_n \rightarrow \mathbf{x}_i}}{\sigma_i^2 + \sum_{S=1}^{N_S} \pi_S} \quad (28)$$

where σ_i^2 stands for the receiver noise power at CR U_i , $p_n \in (0, p_n^{\max}]$ the transmission power of U_n , and π_S the received power from PU transmitter $S = 1, \dots, N_S$. As CR and PU nodes do not generally cooperate, interfering powers $\{\pi_S\}$ are not known. However, their statistics collected by sensing algorithms and CG cartography [cf. (15)] can be used instead. Exploiting the Fenton-Wilkinson method (Fenton, 1960), the distribution of SINRs $\{\gamma_{\mathbf{x}_n \rightarrow \mathbf{x}_i}\}$ can be well approximated as log-normal, with mean and variance of the first- and the second-order moments of $\{g_{\mathbf{x}_n \rightarrow \mathbf{x}_i}\}$ and $\{\pi_S\}$ provided by the CG maps (Dall'Anese et al., 2011b). Let $\bar{\gamma}_{\mathbf{x}_n \rightarrow \mathbf{x}_i}$ denote the SINR threshold, and $\bar{\Gamma}_{\mathbf{x}_n \rightarrow \mathbf{x}_i} := 10 \log_{10} \bar{\gamma}_{\mathbf{x}_n \rightarrow \mathbf{x}_i}$. Assume that CRs adopt a random access strategy, and let μ_n and \mathcal{I}_{ni} denote the transmission probability of CR U_n and the set of nodes whose transmissions interfere with link $U_n \rightarrow U_j$, respectively. Then, the probability that a packet transmitted from the i -th CR U_n is correctly received by U_i can be expressed as

$$r_{\mathbf{x}_n \rightarrow \mathbf{x}_i} = \prod_{j \in \mathcal{I}_{ni}} (1 - \mu_j) \cdot \Pr\{\gamma_{\mathbf{x}_n \rightarrow \mathbf{x}_i} > \bar{\gamma}_{\mathbf{x}_n \rightarrow \mathbf{x}_i}\} \approx \prod_{j \in \mathcal{I}_{ni}} (1 - \mu_j) \cdot Q\left(\frac{\bar{\Gamma}_{\mathbf{x}_n \rightarrow \mathbf{x}_i} - P_n - m_{\mathbf{x}_n \rightarrow \mathbf{x}_i}}{\sigma_{\mathbf{x}_n \rightarrow \mathbf{x}_i}}\right) \quad (29)$$

where $P_n := 10 \log_{10} p_n$; while mean and standard deviation of the dB-expressed SINR are denoted by $m_{\mathbf{x}_n \rightarrow \mathbf{x}_i}$ and $\sigma_{\mathbf{x}_n \rightarrow \mathbf{x}_i}$, respectively.

Assume that exogenous packet arrivals at node U_n are modeled as a stationary stochastic process with average rate $\rho_n \geq 0$. With λ_n denoting the average rate of packet departures from U_n , and assuming fully-backlogged queues per node (Rao and Ephremides, 1988; Ribeiro et al., 2007), the exogenous traffic rates $\{\rho_n\}$ and $\{\lambda_n\}$ abide by the flow conservation constraints

$$\rho_n = \lambda_n \sum_{i \in \mathcal{N}_{n \rightarrow}} t_{\mathbf{x}_n \rightarrow \mathbf{x}_i} r_{\mathbf{x}_n \rightarrow \mathbf{x}_i} - \sum_{j \in \mathcal{N}_{\rightarrow n}} \lambda_j t_{\mathbf{x}_j \rightarrow \mathbf{x}_n} r_{\mathbf{x}_j \rightarrow \mathbf{x}_n} \quad (30)$$

where $\mathcal{N}_{n \rightarrow} := \{j | r_{\mathbf{x}_n \rightarrow \mathbf{x}_j} > 0, j = 1, \dots, N+1, j \neq n\}$ is the set of nodes that decode U_n 's transmissions with non-zero probability, and $\mathcal{N}_{\rightarrow n} := \{i | r_{\mathbf{x}_i \rightarrow \mathbf{x}_n} > 0, i = 1, \dots, N, i \neq n\}$ the set of nodes that route packets through U_n . For queue stability, it suffices to have $0 \leq \lambda_n \leq \mu_n$, for each CR U_n (Loynes, 1962).

To complete the formulation, consider N_R PU receivers, whose locations $\{\mathbf{y}_R\}$ have been estimated via CG cartography [cf. (16)]. The interference caused to PU R is given by $i_R := \sum_n p_n g_{\mathbf{x}_n \rightarrow \mathbf{y}_R}$, where $g_{\mathbf{x}_n \rightarrow \mathbf{y}_R}$ denotes the channel gain between CR U_n and PU R . Approximate the channel gain $g_{\mathbf{x}_n \rightarrow \mathbf{y}_R}$ as log-normal (Dall'Anese et al., 2011b), with mean and variance provided by the CG map of PU receiver R . Then, defining $\kappa := 0.1 \ln(10)$, the average interference experienced at the PU node R is given by

$$\mathbb{E}\{i_{\mathbf{y}_R}\} = \sum_{n=1}^N \mu_n e^{\kappa P_n + \kappa(G_0 - 10\alpha \log_{10} \|\mathbf{x}_n - \mathbf{y}_R\|_2 - s_{\mathbf{x}_n \rightarrow \mathbf{y}_R}) + \frac{\kappa^2}{2} \sigma_{n \rightarrow R}^2} \quad (31)$$

which must not exceed a predetermined threshold ι_R^{max} .

Based on these development, the statistical routing task is formulated as the following optimization problem:

$$\max_{\substack{P_n \leq P^{max}, \{\rho_n \geq 0\}, \{\mu_n \geq 0\}, \\ \{t_{\mathbf{x}_n \rightarrow \mathbf{x}_i} \geq 0\}, \{\lambda_n \geq 0\}}} \sum_{n=1}^N \mathcal{U}_n(\rho_n) - \sum_{n=1}^N \mathcal{C}_n(P_n) \quad (32a)$$

$$\text{subject to } \rho_n \leq \lambda_n \sum_{j \in \mathcal{N}_{n \rightarrow}} t_{\mathbf{x}_n \rightarrow \mathbf{x}_j} r_{\mathbf{x}_n \rightarrow \mathbf{x}_j} - \sum_{i \in \mathcal{N}_{\rightarrow n}} \lambda_i t_{\mathbf{x}_i \rightarrow \mathbf{x}_n} r_{\mathbf{x}_i \rightarrow \mathbf{x}_n} \quad (32b)$$

$$\sum_{i \in \mathcal{N}_{n \rightarrow}} t_{\mathbf{x}_n \rightarrow \mathbf{x}_i} \leq 1, \quad \lambda_n \leq \mu_n - \epsilon, \quad \mu_n \leq 1 \quad (32c)$$

$$\mathbb{E}\{i_{\mathbf{y}_R}\} \leq \iota_R^{max} \quad (32d)$$

with $\{r_{i \rightarrow n}\}$ given by (29), $\epsilon \ll 1$ ensuring queue stability, and $\mathcal{U}_n(\rho_n)$ and $\mathcal{C}_n(P_n)$ selected to be concave and convex functions, respectively, representing the reward of rate ρ_n and the cost of power P_n . Unfortunately, even without the interference constraint (32d), problem (32) is nonconvex. However, a successive convex approximation approach (Marks and Wright, 1978) can be employed to efficiently find to a Karush-Kuhn-Tucker optimal solution (Dall'Anese and Giannakis, 2012).

To illustrate the attractive features of the resultant routing protocol, consider the simple scenario depicted in Fig. 11, where $N_r = 7$ CR nodes route packets generated at U_1 and U_2 to the destination U_8 . Two PU sources also transmit with power 0 dBW. The path loss coefficients are set to $G_0 = 0$, and $\alpha = 3.5$, and $m = 1$ is used for Nakagami- m fading. Log-normal shadowing is generated with mean 0 and standard deviation 6 dB. The maximum transmit-power for the CR system is $P_n^{max} = 0$ dBW, the noise power 10^{-8} , and the SINR threshold $\bar{\Gamma}_n = -10$ dB. The interference threshold is set to -80 dBW, and the sum of exogenous rates was maximized. Fig. 11(a) depicts the optimal routing probabilities obtained by solving (32). It can be seen that due to the presence of PU links, there is a tendency to route packets generated by U_2 through links $U_4 \rightarrow U_6$ and $U_6 \rightarrow U_7$, rather than choosing the

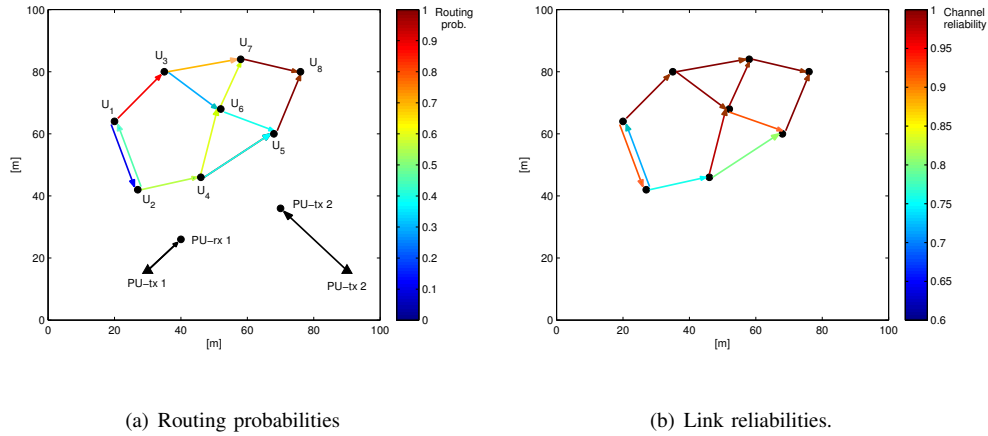


Fig. 11. Cartography-enabled optimal statistical routing.

shortest path $U_2 \rightarrow U_4 \rightarrow U_5 \rightarrow U_8$. Conversely, packets generated by U_1 are routed through U_3 and U_7 with high probability, which in this case coincides with the shortest path. As can be noticed from Fig. 11(b), links to and from U_4 and U_5 manifest lower decoding capability compared to links that are farther from the PU system. This is not only due to the detrimental effect of PU interference on the SINRs, but also due to the fact that U_4 and U_5 are confined to use a lower transmit-power in order to protect PU receivers from harmful interference.

V. CONCLUSIONS

Spectrum sensing at the PHY and MAC layers of CR networks, as well as its cross-layer design and application have been overviewed in this tutorial. At the PHY layer, the basic sensing task was to detect the presence of PU transmitters, for which collaboration of multiple CRs was seen effective to alleviate the challenges due to fading and shadowing effects. It has been also argued that a holistic characterization of the RF environment in which the CR network operates is of great importance for efficient and quality-assuring network design and adaptation. Various signal processing and learning techniques were employed to develop RF cartography algorithms to capture the spatio-temporal-spectral RF environment. At the MAC layer, the key issue was to schedule the per-band sensing operations over the wide bandwidth using limited sensing resources, based on estimated traffic patterns and accumulated sensing history. Cross-layer issues in sensing aimed to strike an optimal trade-off between sensing accuracy and system objectives. The rich cognition of the operating environment obtained via sensing holds a great potential for robust and efficient network operation, which can be realized through cross-layer design.

REFERENCES

- A. Abbagnale and F. Cuomo. Gymkhana: a connectivity-based routing scheme for cognitive radio ad hoc networks. In *Proc. of IEEE INFOCOM*, San Diego, CA, Mar. 2010.
- P. Agrawal and N. Patwari. Correlated link shadow fading in multi-hop wireless network. *IEEE Trans. Wireless Commun.*, 8(8):4024–4036, Aug. 2009.
- S. Ahmad, M. Liu, T. Javidi, Q. Zhao, and B. Krishnamachari. Optimality of myopic sensing in multichannel opportunistic access. *IEEE Trans. Info. Theory*, 55(9):4040–4050, September 2009.
- I. F. Akyildiz, B. F. Lo, and R. Balakrishnan. Cooperative spectrum sensing in cognitive radio networks: A survey. *Elsevier Physical Communication*, 4(1):40–62, Mar. 2011.
- A. B. H. Alaya-Feki, S. B. Jemaa, B. Sayrac, P. Houze, and E. Moulines. Informed spectrum usage in cognitive radio networks: interference cartography. In *Proc. of the PIMRC Conf.*, pages 1–5, Cannes, France, Sep. 2008.
- J. A. Bazerque and G. B. Giannakis. Distributed spectrum sensing for cognitive radio networks by exploiting sparsity. *IEEE Trans. Sig. Proc.*, 58(3):1847–1862, Mar. 2010.
- J. A. Bazerque, G. Mateos, and G. B. Giannakis. Group-Lasso on splines for spectrum cartography. *IEEE Trans. Sig. Proc.*, 59(10):4648–4663, Oct. 2011.
- D. P. Bertsekas. *Dynamic Programming and Optimal Control*, volume 1. Athena Scientific, Belmont, MA, 2nd edition, 2000.
- M. Bishop. *Pattern Recognition and Machine Learning*. Springer-Verlag, New York, 2006.
- V. Blaschke, T. Renk, and F. K. Jondral. A cognitive radio receiver supporting wide-band sensing. In *Proc. of Intl. Conf. on Commun.*, pages 499–503, Beijing, China, May 2008.
- P. J. Brockwell and R. A. Davis. *Introduction to Time Series and Forecasting*. Springer-Verlag, New York, 2nd edition, 2006.
- D. Cabric, S. M. Mishra, and R. W. Brodersen. Implementation issues in spectrum sensing for cognitive radios. In *Proc. of the 38th Asilomar Conf. on Signals, Systems and Computers*, volume 1, pages 772–776, Pacific Grove, CA, Mar. 2005.
- E. J. Candès and Y. Plan. Near-ideal model selection by ℓ_1 minimization. *Annals of Statistics*, 37(5A):2145–2177, Oct. 2009.

- S. Chaudhari, V. Koivunen, and H. V. Poor. Autocorrelation-based decentralized sequential detection of OFDM signals in cognitive radios. *IEEE Trans. Sig. Proc.*, 57(7):2690–2700, Jul. 2009.
- S. S. Chen, D. L. Donoho, and M. A. Saunders. Atomic decomposition by basis pursuit. *SIAM J. Scientific Computing*, 20(1):33–61, 1998.
- Y. Chen, Q. Zhao, and A. Swami. Joint design and separation principle for opportunistic spectrum access in the presence of sensing errors. *IEEE Trans. Info. Theory*, 54(5):2053–2071, May 2008.
- G. Cheng, W. Liu, Y. Li, and W. Cheng. Spectrum aware on-demand routing in cognitive radio networks. In *Proc. of the IEEE DySPAN Conf.*, pages 571–574, Dublin, Ireland, Apr. 2007.
- H. T. Cheng and W. Zhuang. Simple channel sensing order in cognitive radio networks. *IEEE J. Sel. Areas Commun.*, 29(4):676–688, April 2011.
- K. W. Choi, W. S. Jeon, and D. G. Jeong. Sequential detection of cyclostationary signal for cognitive radio systems. *IEEE Trans. Wireless Commun.*, 8(9):4480–4485, Sep. 2009.
- K. R. Chowdhury and I. F. Akyildiz. CRP: A routing protocol for cognitive radio ad hoc networks. *IEEE J. Sel. Areas Commun.*, 29(4):794–802, Apr. 2011.
- C. Cordeiro, K. Challapali, D. Birru, and N. Sai Shankar. IEEE 802.22: the first worldwide wireless standard based on cognitive radios. In *Proc. of the 1st IEEE Int'l. Symp. on New Frontiers in Dynamic Spectrum Access Networks*, pages 328–337, November 2005.
- D. De Couto, D. Aguayo, J. Bicket, and R. Morris. A high-throughput path metric for multi-hop wireless routing. In *Proc. Int. ACM Conf. Mobile Computing, Networking*, pages 134–156, San Diego, CA, Sep. 2003.
- E. Dall'Anese, J. A. Bazerque, and G. B. Giannakis. Group sparse Lasso for cognitive network sensing robust to model uncertainties and outliers. *Elsevier Physical Commun.*, 5(1):161–172, Sep. 2012.
- E. Dall'Anese and G. B. Giannakis. Statistical routing for multihop wireless cognitive networks. *IEEE J. Sel. Areas Commun.*, 30(11), Nov. 2012. (to appear).
- E. Dall'Anese, S.-J. Kim, and G. B. Giannakis. Channel gain map tracking via distributed Kriging. *IEEE Trans. Veh. Technol.*, 60(3):1205–1211, Mar. 2011a.
- E. Dall'Anese, S.-J. Kim, G. B. Giannakis, and S. Pupolin. Power control for cognitive radio networks under channel uncertainty. *IEEE Trans. Wireless Commun.*, 10(10):3541–3551, Oct. 2011b.

- J. Duchon. *Splines Minimizing Rotation-Invariant Semi-norms in Sobolev Spaces*. Springer-Verlag, Berlin, 1977.
- R. Fan and H. Jiang. Channel sensing-order setting in cognitive radio networks: A two-user case. *IEEE Trans. Veh. Technol.*, 58(9):4997–5008, November 2009.
- R. Fan and H. Jiang. Optimal multi-channel cooperative sensing in cognitive radio networks. *IEEE Trans. Wireless Commun.*, 9(3):1128–1138, Mar. 2010.
- FCC Spectrum Policy Task Force. Report of the spectrum efficiency working group, Nov. 2002. URL <http://www.fcc.gov/sptf/reports.html>.
- L. F. Fenton. The sum of lognormal probability distributions in scatter transmission systems. *IRE Trans. Commun. Syst.*, 8(1):57–67, Mar. 1960.
- G. Ganesan and Y. Li. Cooperative spectrum sensing in cognitive radio networks. In *Proc. of the IEEE DySPAN Conf.*, pages 137–143, Baltimore, MD, Nov. 2005.
- G. Ganesan, Ye Li, B. Bing, and Shaoqian Li. Spatiotemporal sensing in cognitive radio networks. *IEEE J. Sel. Areas Commun.*, 26(1):5–12, Jan. 2008.
- S. Geirhofer, L. Tong, and B. M. Sadler. Dynamic spectrum access in the time domain: Modeling and exploiting white space. *IEEE Commun. Mag.*, 45(5):66–72, May 2007.
- S. Geirhofer, L. Tong, and B. M. Sadler. A sensing-based cognitive coexistence method for interfering infrastructure and *ad hoc* systems. *Wireless Commun. and Mobile Comput.*, 10(1):16–30, Jan. 2010.
- A. Ghasemi and E. S. Sousa. Spectrum sensing in cognitive radio networks: the cooperation-processing tradeoff. *Wireless Commun. Mobile Comput.*, 7(9):1049–1060, Nov. 2007.
- A. Goldsmith. *Wireless communications*. Cambridge University Press, 2005.
- A. Goldsmith, L. J. Greenstain, and G. J. Foschini. Error statistics of real-time power measurements in cellular channels with multipath and shadowing. *IEEE Trans. Veh. Technol.*, 43(3):439–446, Aug. 1994.
- F. Graziosi and F. Santucci. A general correlation model for shadow fading in mobile radio systems. *IEEE Commun. Lett.*, 6(3):102–104, Mar. 2002.
- M. Gudmundson. Correlation model for shadow fading in mobile radio systems. *Elec. Lett.*, 27(23):2145–2146, Nov. 1991.
- M. Haenggi. On routing in random rayleigh fading networks. *IEEE Trans. Wireless Commun.*, 4(4):1553–1562,

- Jul. 2005.
- T. Hastie, R. Tibshirani, and J. Friedman. *The Elements of Statistical Learning*. Springer-Verlag, New York, NY, 2nd edition, 2009.
- S. Haykin. Cognitive radio: brain-empowered wireless communications. *IEEE J. Sel. Areas Commun.*, 23(2): 201–220, Feb. 2005.
- A. T. Hoang, Y.-C. Liang, D. Wong, Y. Zeng, and R. Zhang. Opportunistic spectrum access for energy-constrained cognitive radios. *IEEE Trans. Wireless Commun.*, 8(3):1206–1211, March 2009.
- X. Hong, C.-X. Wang, and J. Thompson. Interference modeling of cognitive radio networks. In *Proc. of the IEEE Veh. Tech. Conf.*, pages 1851–1855, Singapore, May 2008.
- W. Hu, D. Willkomm, M. Abusubaih, J. Gross, G. V. Lantis, M. Gerla, and A. Wolisz. Dynamic frequency hopping communities for efficient IEEE 802.22 operation. *IEEE Commun. Mag.*, 45(5):80–87, May 2007.
- S. Huang, X. Liu, and Z. Ding. Optimal transmission strategies for dynamic spectrum access in cognitive radio networks. *IEEE Trans. Mob. Comput.*, 8(12):1636–1648, December 2009.
- J. Jia, Q. Zhang, and X. Shen. HC-MAC: a hardware-constrained cognitive MAC for efficient spectrum management. *IEEE J. Sel. Areas Commun.*, 26(1):106–117, Jan. 2008.
- H. Jiang, L. Lai, R. Fan, and H. V. Poor. Optimal selection of channel sensing order in cognitive radio. *IEEE Trans. Wireless Commun.*, 8(1):297–307, Jan. 2009.
- H. Khalife, S. Ahuja, N. Malouch, and M. M. Krunz. Probabilistic path selection in opportunistic cognitive radio networks. In *Proc. of IEEE Glob. Telecom. Conf.*, New Orleans, LA, Dec. 2010.
- H. Kim and K. G. Shin. Efficient discovery of spectrum opportunities with MAC-layer sensing in cognitive radio networks. *IEEE Trans. Mob. Comput.*, 7(5):533–545, May 2008a.
- H. Kim and K. G. Shin. Fast discovery of spectrum opportunities in cognitive radio networks. In *Prof. of the IEEE Symposium on New Frontiers in Dynamic Spectrum Access Networks*, pages 1–12, October 2008b.
- S.-J. Kim, E. Dall’Anese, and G. B. Giannakis. Cooperative spectrum sensing for cognitive radios using Krige Kalman filtering. *IEEE J. Sel. Topics Sig. Proc.*, 5:24–36, Feb. 2011a.
- S.-J. Kim and G. B. Giannakis. Rate-optimal and reduced-complexity sequential sensing algorithms for cognitive OFDM radios. *EURASIP J. Adv. Sig. Proc.*, 2009. Article ID 421540, 11 pages.

- S.-J. Kim and G. B. Giannakis. Sequential and cooperative sensing for multi-channel cognitive radios. *IEEE Trans. Sig. Proc.*, 58(8):4239–4253, Aug. 2010.
- S.-J. Kim, G. Li, and G. B. Giannakis. Multi-band cognitive radio spectrum sensing for quality-of-service traffic. *IEEE Trans. Wireless Commun.*, 10(10):3506–3515, Oct. 2011b.
- K. Kumaran, S. E. Golowich, and S. Borst. Correlated shadow-fading in wireless networks and its effect on call dropping. *Wireless Networks*, 8(1):61–71, Jan. 2002.
- N. Kundargi and A. Tewfik. Hierarchical sequential detection in the context of dynamic spectrum access for cognitive radios. In *Proc. of the Intl. Conf. on Electr., Circuits and Syst.*, pages 514–517, Marrakech, Morocco, Dec. 2007.
- L. Lai, H. El Gamal, H. Jiang, and H. V Poor. Cognitive medium access: Exploration, exploitation, and competition. *IEEE Trans. Mob. Comput.*, 10(2):239–253, February 2011.
- B. Le, T. W. Rondeau, J. H. Reed, and C. W. Bostian. Analog-to-digital converters. *IEEE Sig. Proc. Mag.*, 22(6):69–77, Nov. 2005.
- X. Li and S. A Zekavat. Traffic pattern prediction and performance investigation for cognitive radio systems. In *Proc. of the IEEE Wireless Commun. and Net. Conf.*, pages 894–899, April 2008.
- X. Li, Q. Zhao, X. Guan, and L. Tong. Optimal cognitive access of Markovian channels under tight collision constraints. *IEEE J. Sel. Areas Commun.*, 29(4):746–756, April 2011.
- Y.-C. Liang, Y. Zeng, E. C. Y. Peh, and T. Hoang. Sensing-throughput tradeoff for cognitive radio networks. *IEEE Trans. Wireless Commun.*, 7(4):1326–1337, Apr. 2008.
- K. Liu and Q. Zhao. Indexability of restless bandit problems and optimality of Whittle index for dynamic multichannel access. *IEEE Trans. Info. Theory*, 56(11):5547–5567, November 2010.
- X. Long, X. Gan, Y. Xu, J. Liu, and M. Tao. An estimation algorithm of channel state transition probabilities for cognitive radio systems. In *Proc. of the IEEE Intl. Conf. on Cognitive Radio Oriented Wireless Netw. and Commun. (CrownCom)*, pages 1–4, May 2008.
- R. Loynes. The stability of a queue with non-independent interarrival and service times. *Mathematical Proc. of the Cambridge Philosophical Society*, 58:497–520, 1962.
- J. Lunden, V. Koivunen, A. Huttunen, and H. V. Poor. Collaborative cyclostationary spectrum sensing for cognitive

- radio systems. *IEEE Trans. Sig. Proc.*, 57(11):4182–4195, Nov. 2009.
- J. Ma, G. Zhao, and Y. Li. Soft combination and detection for cooperative spectrum sensing in cognitive radio networks. *IEEE Trans. Wireless Commun.*, 7(11):4502–4507, Nov. 2008.
- S. Maleki, A. Pandharipande, and G. Leus. Energy-efficient distributed spectrum sensing for cognitive sensor networks. *IEEE Sensors Journal*, 11(3):565–573, Mar. 2011.
- K. V. Mardia, C. Goodall, E. J. Redfern, and F. J. Alonso. The Kriged Kalman filter. *Test*, 7(2):217–285, Dec. 1998.
- B. R. Marks and G. P. Wright. A general inner approximation algorithm for nonconvex mathematical programs. *Oper. Res.*, 26(4):681–683, Jul.-Aug. 1978.
- J. Mitola III and G. Q. Maguire, Jr. Cognitive radio: making software radios more personal. *IEEE Pers. Commun.*, 6(4):13–18, Aug. 1999.
- D. A. Castanon. Approximate dynamic programming for sensor management. In *Proc. of the 36th Conf. on Decision and Contr.*, volume 2, pages 1202–1207, San Diego, CA, Dec. 1997.
- C. Oestges, N. Czink, B. Bandemer, P. Castiglione, F. Kaltenberger, and A. J. Paulraj. Experimental characterization and modeling of outdoor-to-indoor and indoor-to-indoor distributed channels. *IEEE Trans. Veh. Technol.*, 59:2253–2265, Jun. 2010.
- P. Pawelczak, K. Nolan, L. Doyle, S. W. Oh, and D. Cabric. Cognitive radio: Ten years of experimentation and development. *IEEE Commun. Mag.*, 49(3):90–100, Mar. 2011.
- I. Pefkianakis, S. H. Y. Wong, and S. Lu. SAMER: Spectrum aware mesh routing in cognitive radio networks. In *Proc. of IEEE DySPAN*, Chicago, IL, Oct. 2008.
- Z. Quan, S. Cui, and A. H. Sayed. Optimal linear cooperation for spectrum sensing in cognitive radio networks. *IEEE J. Sel. Topics Sig. Proc.*, 2(1):28–40, Feb. 2008.
- Z. Quan, S. Cui, A. H. Sayed, and H. V. Poor. Optimal multiband joint detection for spectrum sensing in cognitive radio networks. *IEEE Trans. Sig. Proc.*, 57(3):1128–1140, Mar. 2009.
- R. Rao and A. Ephremides. On the stability of interacting queues in a multi-access system. *IEEE Trans. Info. Theory*, 34:918–930, Sep. 1988.
- T. S. Rappaport. *Wireless Communications: Principles & Practice*. Prentice Hall, 1996.

- A. Ribeiro, Z.-Q. Luo, N. Sidiropoulos, and G. B. Giannakis. Modelling and optimization of stochastic routing for wireless multihop networks. In *Proc. IEEE Int. Conf. on Computer Commun.*, pages 1748–1756, Anchorage, AK, May 2007.
- A. Ribeiro, N. Sidiropoulos, and G. B. Giannakis. Optimal distributed stochastic routing algorithms for wireless multihop networks. *IEEE Trans. Wireless Commun.*, 7(11):4261–4272, Nov. 2008.
- B. D. Ripley. *Spatial Statistics*. John Wiley & Sons, 1981.
- S. Sengupta, S. Brahma, M. Chatterjee, and N. Sai Shankar. Enhancements to cognitive radio based IEEE 802.22 air-interface. In *Proc. of the IEEE ICC Conf.*, pages 5155–5160, June 2007.
- Y. Shi and Y. T. Hou. A distributed optimization algorithm for multi-hop cognitive radio networks. In *Proc. of the IEEE INFOCOM Conf.*, pages 1292–1300, Phoenix, AZ, Apr. 2008.
- H.-P. Shiang and M. van der Schaar. Distributed resource management in multihop cognitive radio networks for delay-sensitive transmission. *IEEE Trans. Veh. Technol.*, 58(2):941–953, Feb. 2009.
- G. L. Stüber. *Principles of Mobile Communication*. Kluwer Academic Publishers, Boston, MA, 2nd edition, 2001.
- R. Tandra and A. Sahai. SNR walls for signal detection. *IEEE J. Sel. Topics in Sig. Proc.*, 2(1):4–17, Feb. 2008.
- Z. Tian and G. B. Giannakis. Compressed sensing for wideband cognitive radios. In *Proc. of the IEEE ICASSP Conf.*, volume 4, pages 1357–1360, Honolulu, HI, Apr. 2007.
- R. Tibshirani. Regression shrinkage and selection via the lasso. *J. Royal Statistical Society, Series B*, 58(1):267–288, 1996.
- J. Unnikrishnan and V. V. Veeravalli. Cooperative sensing for primary detection in cognitive radio. *IEEE J. Sel. Topics in Sig. Proc.*, 2(1):18–27, Feb. 2008.
- J. Unnikrishnan and V. V. Veeravalli. Algorithms for dynamic spectrum access with learning for cognitive radio. *IEEE Trans. Sig. Proc.*, 58(2):750–760, February 2010.
- G. Wahba. *Spline Models for Observational Data*. SIAM, Philadelphia, 1990.
- B. Wang, K. J. R. Liu, and T. C. Clancy. Evolutionary cooperative spectrum sensing game: how to collaborate? *IEEE Trans. Commun.*, 58(3):890–900, Mar. 2010.
- J. Wang, P. Urriza, Y. Han, and D. Cabric. Weighted centroid localization algorithm: Theoretical analysis and distributed implementation. *IEEE Trans. Wireless Commun.*, 10(10):3403–3413, Oct. 2011.

- R. Wang, V. K. N. Lau, L. Lv, and B. Chen. Joint cross-layer scheduling and spectrum sensing for OFDMA cognitive radio systems. *IEEE Trans. Wireless Commun.*, 8(5):2410–2416, May 2009.
- Z. Wang, E. K. Tameh, and A. Nix. Simulating correlated shadowing in mobile multihop relay/ad hoc networks. Technical Report IEEE C802.16j-06/060, IEEE 802.16 Broadband Wireless Access Working Group, Jul. 2006.
- C. K. Wikle and N. Cressie. A dimension-reduced approach to space-time Kalman filtering. *Biometrika*, 86(4): 815–829, 1999.
- D. Willkomm, M. Bohge, D. Hollos, J. Gross, and A. Wolisz. Double hopping: A new approach for dynamic frequency hopping in cognitive radio networks. In *Proc. of the IEEE Intl. Symp. on Personal, Indoor and Mobile Radio Commun. (PIMRC)*, pages 1–6, September 2008.
- C. Xin, L. Ma, and C.-C. Shen. A path-centric channel assignment framework for cognitive radio wireless networks. *Mobile Net. Appl. (Kluwer)*, 13(5):463–476, Oct. 2008.
- Y. Xin, H. Zhang, and S. Rangarajan. SSCT: A simple sequential spectrum sensing scheme for cognitive radio. In *Proc. of the GLOBECOM Conf.*, pages 1–6, Honolulu, HI, Nov.–Dec. 2009.
- S. Yarkan and H. Arslan. Binary time series approach to spectrum prediction for cognitive radio. In *Proc. of the IEEE Veh. Technol. Conf.*, pages 1563–1567, October 2007.
- M. Yuan and Y. Lin. Model selection and estimation in regression with grouped variables. *J. Royal Statistical Society*, 68:49–67, Feb. 2006.
- F. Zeng, C. Li, and Z. Tian. Distributed compressive spectrum sensing in cooperative multihop cognitive networks. *IEEE J. Sel. Topics Sig. Proc.*, 5(1):37–48, Feb. 2011.
- R. Zhang. On peak versus average interference power constraints for protecting primary users in cognitive radio networks. *IEEE Trans. Wireless Commun.*, 8(4):2112–2120, Apr. 2009.
- W. Zhang, R. Mallik, and K. Letaief. Optimization of cooperative spectrum sensing with energy detection in cognitive radio networks. *IEEE Trans. Wireless Commun.*, 8(12):5761–5766, Dec. 2009.
- Q. Zhao, S. Geirhofer, L. Tong, and B. M. Sadler. Opportunistic spectrum access via periodic channel sensing. *IEEE Trans. Sig. Proc.*, 56(2):785–796, February 2008a.
- Q. Zhao, B. Krishnamachari, and K. Liu. On myopic sensing for multi-channel opportunistic access: structure, optimality, and performance. *IEEE Trans. Wireless Commun.*, 7(12):5431–5440, December 2008b.

- Q. Zhao and B. M. Sadler. A survey of dynamic spectrum access. *IEEE Sig. Proc. Mag.*, 24(3):79–89, May 2007.
- Q. Zhao and A. Swami. A decision-theoretic framework for opportunistic spectrum access. *IEEE Wireless Commun.*, 14(4):14–20, August 2007.
- Q. Zhao, L. Tong, A. Swami, and Y. Chen. Decentralized cognitive MAC for opportunistic spectrum access in ad hoc networks: A POMDP framework. *IEEE J. Sel. Areas Commun.*, 25(3):589–600, April 2007.
- Q. Zhao and J. Ye. When to quit for a new job: quickest detection of spectrum opportunities in multiple channels. In *Proc. of the MILCOM Conf.*, San Diego, CA, Nov. 2008.
- H. Zhu, G. Leus, and G. B. Giannakis. Sparsity-cognizant total least-squares for perturbed compressive sampling. *IEEE Trans. Sig. Proc.*, 59:2002–2016, May 2011.